

Steel mice have a defect in the hematopoietic micro-environment, or the niche, where marrow stromal cells constitute (Harrison and Russell, 1972).

Bone marrow stromal cells are capable of differentiating into adipocytes, endothelial cells, chondrocytes, and osteoblasts (Pittenger et al., 1999). They are also capable of transdifferentiating into cardiomyocytes, skeletal myocytes, and neurons when exposed to inducers in vitro and in vivo (Umezawa et al., 1992; Makino et al., 1999; Kohyama et al., 2001; Takeda et al., 2004; Mori et al., 2005; Terai et al., 2005). Previous studies on the role of stromal cells in supporting HSCs have mainly been based on in vitro culture. The trabecular area of cancellous bone is the primary site of HSCs. They arise next to the inner surface of bone, and then migrate towards the blood vessels at the center of the bone marrow cavity as they mature. Since the 1970s, efforts to characterize the HSC niche have been focusing on developing systems in vitro that mimic some of the features of stem cell–niche interactions in vivo, and single clones of stromal cells have been found to be capable of supporting HSC self-renewal and differentiation in vivo (Okada et al., 1991, 1992). Osteoblastic marrow stromal cells are a regulatory component of the HSC niche in vivo that influences stem cell function, and some stromal cell clones are part of the bone-forming 'osteoblastic' lineage, which is consistent with a notion that osteoblasts may be a component of the HSC niche in vivo (Lord, 1990; Yoshimoto et al., 2003).

In the present study, we demonstrate that KUSA-A1 osteoblasts, whose number has been increased by local injection into the tissues, support an increase in the number of HSCs in both bone marrow and peripheral blood as a result of an increase in size of the microenvironment or niche in vivo. We provide in vivo evidence that shows an extra osteogenic process independent from that in the normal bone affects the reproduction of stem cells.

MATERIALS AND METHODS

Mice and their major histocompatibility complex (MHC) Class I

BALB/c nu/nu (H-2d), BALB/c (H-2d), C57BL/6N (H-2b), and C3H/He (H-2k) mice were obtained from Clea Japan Inc (Tokyo, Japan).

Cell lines and cell culture

KUSA-A1 cells, that was derived from a C3H/He mouse, were maintained in the M061101 medium (okada@med-shirotori.co.jp, MED SHIROTORI Co., Ltd., Tokyo) on 100 mm culture dishes (Falcon 3003; Becton Dickinson Labware, Bedford, MA) at 37°C under a humidified atmosphere of 5% CO₂. ST-2 cells were obtained from the RIKEN cell bank, Japan, and were maintained in RPMI 1640 (Invitrogen Corporation, Auckland, New Zealand) supplemented with 10% FCS and 10⁻⁶M of 2-ME (GIBCO BRL) at 37°C under a humidified atmosphere of 5% CO₂ in air.

Cell transplantation

Freshly scraped confluent cells (5 × 10⁶) were subcutaneously implanted into BALB/c nu/nu mice (Clea). These animals were sacrificed by cervical dislocation between 3 and 10 weeks after implantation.

Antibodies

Phycoerythrin (PE)-conjugated antibodies to CD4, CD8, CD3, B220, Mac-1, Gr-1, and Tre119 (Pharmingen, San Diego, CA), fluorescein isothiocyanate (FITC)-conjugated antibody to CD34, H-2k (Pharmingen), allophycocyanin (APC)-conju-

gated antibody to c-kit (Pharmingen), Sca-1 biotinate antibody (Pharmingen), and antibody to CD16/32 (Fc III/II receptor; 1: 100; Fcblock; Pharmingen) were used for flow cytometric analysis.

Flow cytometric analysis

The monoclonal antibodies (mAbs) were either biotinylated or fluoresceinated. Biotinylated mAbs were detected with streptavidin-conjugated Red 613 (Invitrogen Corporation). Cells were incubated for 30 min on ice with CD16/32 (Fc III/II receptor; 1: 100; Fcblock) before staining with the first antibody. Cells were stained with the first antibody, incubated for 30 min on ice, and then washed twice with washing buffer. The secondary antibody was added, and after incubating the cells for 30 min on ice, they were washed twice with washing buffer and suspended in washing buffer. KUSA-A1 cell suspensions were prepared from monolayer cultures by exposure to trypsin (0.02% for 3 min at 37°C), followed by two washes in cold PBS plus 2% FCS and 0.01% sodium azide. After staining with a series of monoclonal antibodies according to manufacturer's protocol, cells were analyzed by fluorescence-activated cell sorter (FACS) with the FACS vantage system (Becton Dickinson, San Jose, CA).

Colony-forming unit in spleen (CFU-S) assay of hematopoietic cells obtained from ectopic bone

Freshly scraped confluent KUSA-A1 cells (5 × 10⁶) were subcutaneously implanted into BALB/c nu/nu mice (Clea). Hematopoietic cells were obtained from ectopic bone marrow generated by KUSA-A1 cells, and were assayed for CFU-S. Bone marrow cells (5 × 10⁵) were implanted into lethally irradiated BALB/c mice, and the number of colonies (Day 12 CFU-S) was counted 12 days after transplantation. Day 12 CFU-S including erythrocytic, granulocytic, megakaryocytic, and lymphocytic lineages are derived from multipotent HSCs and are more potent in terms of repopulating ability than day 8 CFU-S.

Soft X ray system

BALB nu/nu mice were examined by whole body soft X-ray radiography at 25.0 kV and 3.0 mA for 10 sec (SRO-IM50, Sofron, Tokyo) with X-ray RX film (Fuji Photofilm GmbH, Düsseldorf, Germany).

RESULTS

Induction of hematopoiesis by KUSA-A1 cells

When KUSA-A1 cells were implanted into the subcutaneous tissue, solid hard masses (Fig. 1A) were detected 5 weeks later as electron-dense nodules by soft X-ray analysis (Fig. 1B) at all implantation sites, that is, in the dermal tissue right beneath the cutaneous muscle. Histological examination revealed that the implanted cells survived, and some of them showed mitotic figures (Fig. 1C(a)). At 2 weeks following implantation, an osteogenic matrix was formed in the interstitium, but its matrix formation was still scanty (Fig. 1C(b)). And marked formation of capillary vessels containing erythrocytes in their lumen was observed. At 3 weeks, dense immature bone trabeculae with prominent vascular formation and osteoclast induction were seen (Fig. 1C(c)). By 4 weeks, mature bone trabeculae and sinusoids formed (Fig. 1C(d)), and there were mature granulocytic cells in the marrow space. Hematopoiesis began by 3–5 weeks after implantation.

To determine whether the size of the bone generated by KUSA-A1 cells depends on the implanted cell number, we implanted different numbers of KUSA-A1 cells into subcutaneous tissue (Fig. 1D). The results showed that bone size was clearly depending on the number of cells implanted. Nevertheless, hematopoiesis occurred regardless of the number of cells implanted and bone size.

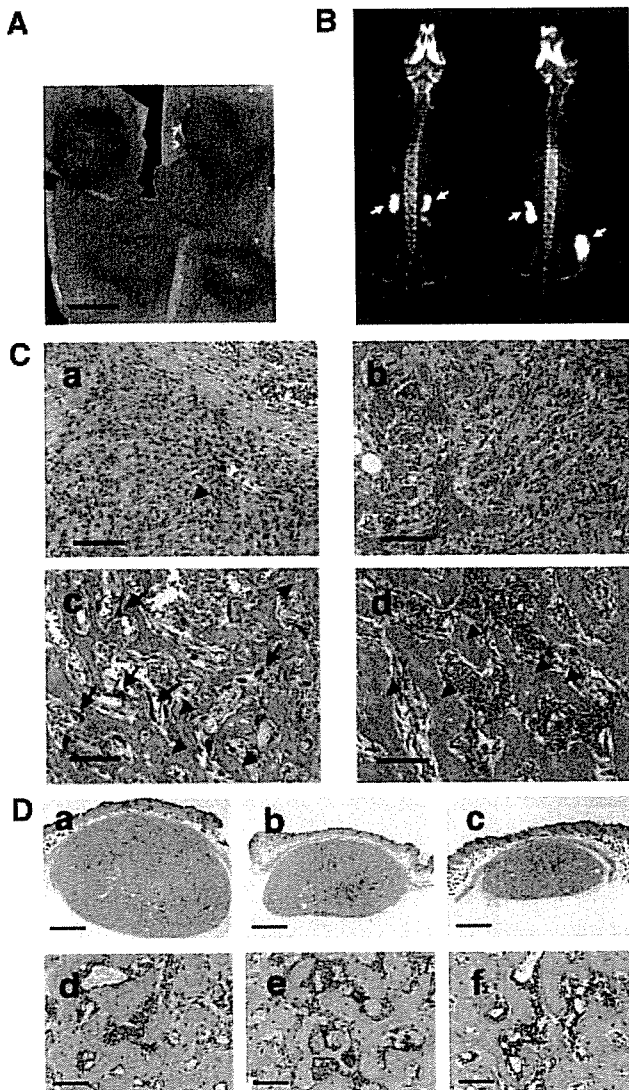


Fig. 1. Time course analysis of hematopoietic induction by KUSA-A1-induced membranous osteogenesis. KUSA-A1 cells were implanted into the subcutaneous tissue of BALB/c nu/nu mice at a density of 2×10^7 cells/200 μ l. **A:** Macroscopic view of bone formation at 5 weeks after KUSA-A1 cell injection. **B:** Soft X-ray image of a bone nodule formed by KUSA-A1 cells 5 weeks after implantation. **C:** Histopathological examination of induction of hematopoiesis and bone formation at 1 (a), 2 (b), 3 (c), and 4 (d) weeks after KUSA-A1 cell implantation. The mitotic figure of the implanted cell is indicated by an arrowhead (a). Note that numerous osteoclasts (c, arrows) as well as osteoblasts and osteocytes (c, arrowheads) were detected at 3 weeks after implantation. Mature osteocytes were observed at 4 weeks (d, arrowheads). Hematoxylin and eosin stain. Scale bars: 10 mm (A), 230 μ m (C–F). **D:** Correlation between the number of cells implanted and the size of the bone nodules. Microscopic view of the KUSA-A1 bone 5 weeks after implantation of 2×10^7 (a, d), 1×10^7 (b, e), or 5×10^6 (c, f) KUSA-A1 cells into subcutaneous tissue. Hematoxylin and eosin stain. Scale bars: 2 mm (a–c), 250 μ m (d), 300 μ m (e), 250 μ m (f).

Expression of major histocompatibility antigen (MHC) after implantation

Marrow stromal cells have been reported to be immunologically tolerant, probably due to lack of transplantation antigen expression. To determine whether KUSA-A1 cells are tolerant when implanted into an allogeneic host, KUSA-A1 cells, which are C3H/He mouse origin, were implanted into BALB/c mice (Fig. 2). Time-course analysis clearly revealed that all of

the cells were rejected and formed no bone, but numerous foreign body giant cells were observed (Fig. 2C,D), suggesting that KUSA-A1 cells are immunogenic in our experimental setting.

To determine alterations in MHC antigens after implantation, flow cytometric analysis was performed on KUSA-A1 cells (Fig. 2E, open peaks) and cultured mesenchymal cells obtained from KUSA-A1-induced ectopic bone (Fig. 2E, closed peaks) in BALB/c nu/nu mice. The KUSA-A1 cells started to express one of the MHC antigens, H-2k, after implantation into BALB/c nu/nu mice, but expression of Sca-1 was downregulated. Expression of Lin (CD3, CD4, CD8, B220, Gr-1, Mac-1, and Ter119), c-kit, and CD34 remained unchanged after implantation.

MHC expression of the hematopoietic cells in the KUSA-A1 cell-induced bone

Morphological analysis showed that hematopoiesis took place in the KUSA-A1-induced ectopic bone (Fig. 3A–E). Megakaryocytes (arrows in Fig. 3D), erythrocytes (Fig. 3D,E), and granulocytes (Fig. 3D,E) were detected as well as osteoblasts (arrows in Fig. 3E) and mature osteocytes (arrowheads in Fig. 4E). The hematopoietic cells isolated from the KUSA-A1 cell-induced ectopic bone expressed the H-2d antigen, implying that they were derived from the host cells and had not differentiated from the implanted KUSA-A1 cells.

Cytokine production by the implanted KUSA-A1 cells may not be attributable to the migration of hematopoietic cells

To determine whether cytokines, that is, interleukin-6, macrophage-colony stimulating factor, stem cell factor, fms-like tyrosine kinase-3 ligand, and thrombopoietin, were produced by the implanted cells and contributed to the hematopoiesis, ELISA analysis was performed on the serum from mice with cell implantation as well as conditioned medium of the KUSA-A1 cultures (Fig. 3F). RT-PCR analysis of cytokine gene expression revealed that the KUSA-A1 cells express CSF-1, thrombopoietin, angiotensinogen, c-kit ligand, leptin, lymphotoxin A and B, IL4, IL5, IL6, IL10, IL12B, IL16, IL17B, IL19, and angiopoietin1 genes (Supplementary Figure 1S) and transcriptome analysis revealed that KUSA-A1 cells express the SDF-1 gene at a high level (a frequency of 1.1×10^{-3}) (Sharov et al., 2003). However, none of the cytokine levels increased in the serum.

Analysis of KSL cells in the femur and the ectopic bone, and CFU-S in the peripheral blood and the ectopic bone

To investigate whether HSCs as well as mature hematopoietic cells migrates into the ectopic bone, the proportion of KSL cells was examined. The proportion was found to be the same, that is, 0.08%, in both the host femur (Fig. 4A) and the KUSA-A1 ectopic bone (Fig. 4B), suggesting that the ectopic bone as well as native bone serves microenvironment for HSCs.

The number of CFU-S were also counted in the host femur, peripheral blood, and KUSA-A1-induced bone marrow (Fig. 4C–E), and were found to account for $11.2 \pm 0.8/1.0 \times 10^5$ the cells in the KUSA-A1-induced ectopic bone (Fig. 4E, right). By day 12 the CFU-S of the host femur had increased from 28.3 ± 6.0 to $35.0 \pm 3.4/10^5$ cells (Fig. 4E, left). At day 12 CFU-S were also detected in the peripheral blood from the mice and

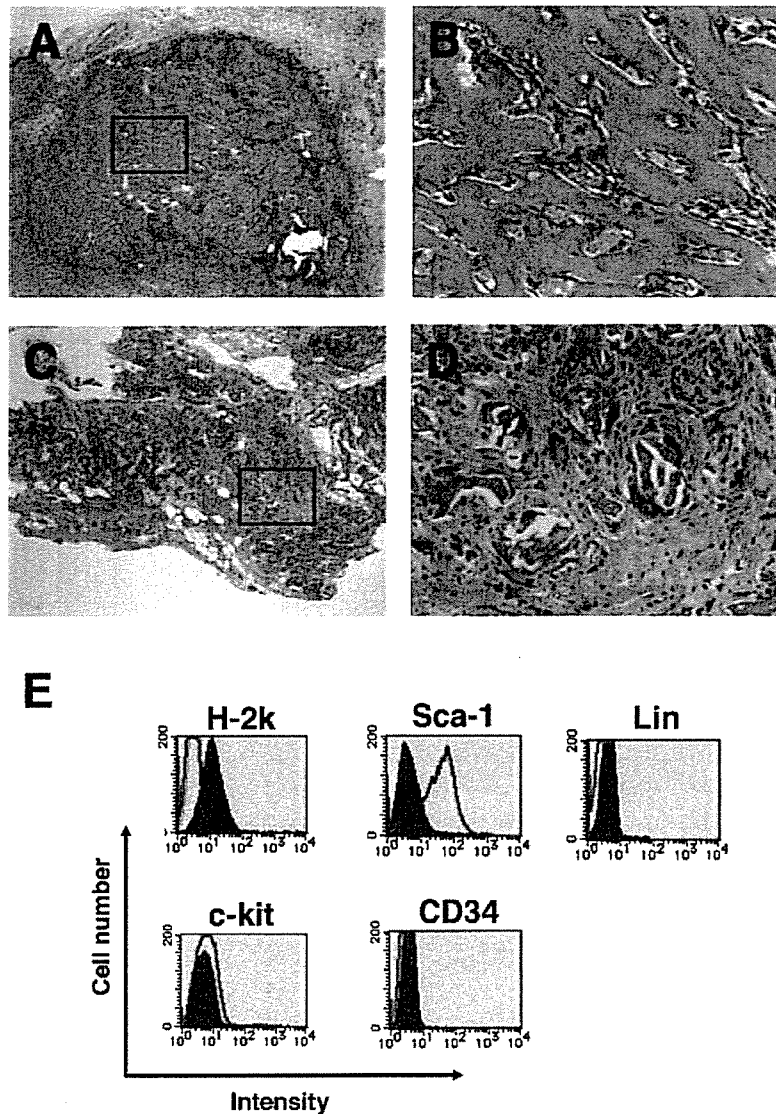


Fig. 2. Rejection of the implanted KUSA-A1 cells in an allogeneic combination. Microscopic view of the generated bone 18 days after the implantation of 5×10^6 KUSA-A1 cells, which were derived from C3H/He mice, into the subcutaneous tissue of syngeneic C3H/He mice (A, B) or allogeneic BALB/c mice (C, D). Hematoxylin and eosin stain. Parts B and D are higher magnifications of A and C, respectively. E: Alterations in cell surface antigens after implantation. Flow

cytometric analysis was performed on KUSA-A1 cells (open peaks) and cultured mesenchymal cells obtained from KUSA-A1 ectopic bone (closed peaks) in BALB/c nu/nu mice. The mesenchymal cells were obtained from the KUSA-A1 ectopic bone, and analyzed by flow cytometry. One of major histocompatibility antigens, H-2k, was upregulated, and Sca-1 antigen was downregulated.

accounted for $7.0 \pm 1.7/10^6$ cells (Fig. 4E, middle). In contrast, no CFU-S was detected in the peripheral blood from the mice without KUSA-A1 cell implantation.

Since the upregulation of HSCs in the femurs from the KUSA-A1 cell-implanted mice was rather surprising to us, the time-course of the KSL cell numbers in the femurs from the mice with KUSA-A1 ectopic bone was investigated (Fig. 4F). The number of KSL cells started to increase at 3 weeks, continued to increase to 0.47% by 5 weeks, returned to the basal level, that is, 0.08% at 6 weeks, and then fell down to 0.07% at 7 weeks, implying that the HSC number is strongly correlated with the process of dynamic membranous osteogenesis at the implanted site.

DISCUSSION

Bone remodeling occurs continuously throughout life, and HSCs may mobilize during this remodeling process.

The finding in this study support such hypothesis that a very specific niche may be functionally enhanced by bone remodeling (Watt and Hogan, 2000), while a stable or static microenvironment does not support hematopoietic mobilization. For example, accelerated bone remodeling by physical exercise and Vitamin D intake trigger increasing mobilization of HSCs. On the other hand, lack of dynamic bone remodeling in bedridden elderly, astronauts, dieters, postmenopausal women, and patients immobilized for long periods results in downregulation of HSCs in bone marrow.

Upregulation of HSCs by "dynamic" membranous ossification of implanted KUSA-A1 osteoblasts

The cell implantation-based strategy employed in this study revealed that increased niche size following subcutaneous implantation of an osteoblast cell line in syngeneic or immunodeficient mice resulted in

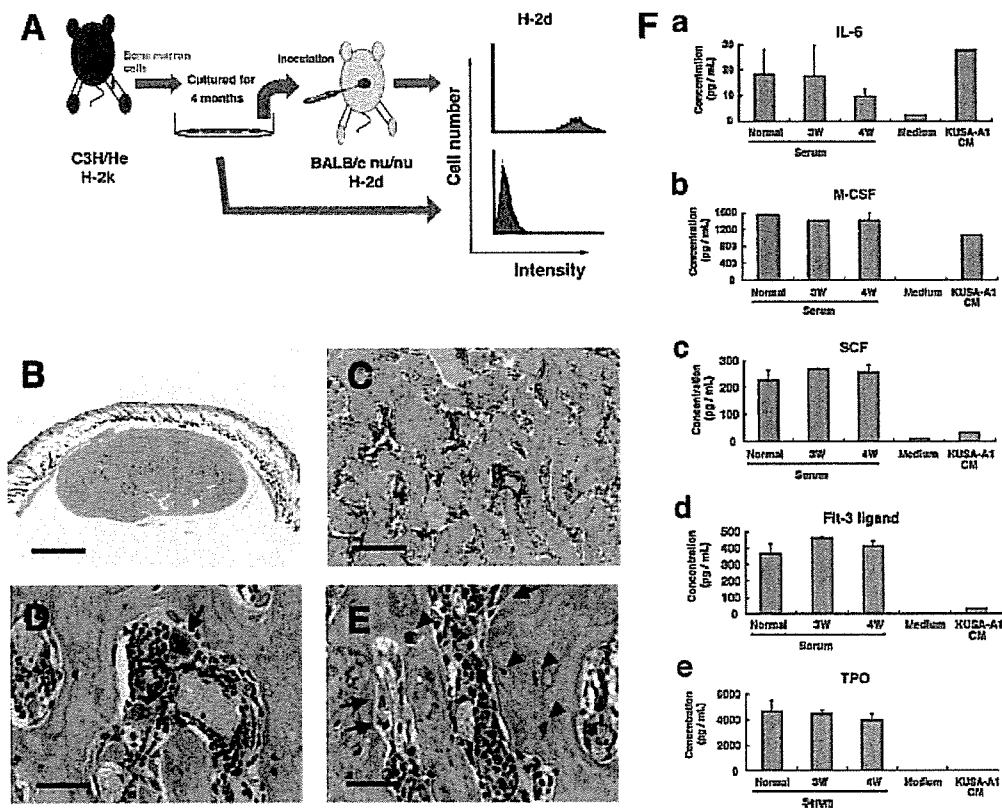


Fig. 3. Hematopoietic cells of host origin in the ectopic bone and serum levels of cytokines after subcutaneous implantation of KUSA-A1 cells. **A**: Flow cytometric analysis of the H-2d antigen in the hematopoietic cells of ectopic bone and KUSA-A1 cells in vitro. The hematopoietic cells in KUSA-A1 bone were examined for expression of the H-2d antigen of the host mice. **B–E**: Histopathological appearance of the hematopoietic cells used for flow cytometric analysis. Tri-lineage cells, that is, megakaryocytes (D, arrows), erythroblasts (D, E),

and granulocytes (E), were observed. Osteoblasts and mature osteocytes are indicated by arrows and arrowheads, respectively (E). Scale bars: 2 mm (B), 400 μ m (C), 100 μ m (D, E). **F**: Serum levels of interleukin-6 (IL-6) (a), macrophage-colony stimulating factor (M-CSF) (b), stem cell factor (SCF) (c), fms-like tyrosine kinase-3 (Flt-3) ligand (d), and thrombopoietin (TPO) (e), measured by the ELISA method. The blood samples were obtained at 5 weeks after implantation.

increases in the HSC population. In the HSC population, both the CFU-S and KSL cells increased. The niche that regulates the generation and differentiation of the HSCs was formed following KUSA-A1 cell implantation, and subsequent membranous ossification in vivo. The enlarged area of niche, that is, the inner surface of bone during the dynamic process of membranous osteogenesis may account for the dramatic upregulation of HSCs in the host bone marrow. Once the osteogenic process is terminated, the number of osteoclasts decreases and no bone is remodeled. Furthermore, the number of the KSL cells returns to the basal level in host bone marrow. These facts suggest a correlation between the osteogenic process (Fig. 1C) and increasing number of KSL cells (Fig. 4F).

The source of the CFU-S in the peripheral blood of the mice implanted with KUSA-A1 osteoblasts may be the bone marrow of (a) the ectopic bone; (b) the host femur; (c) both the ectopic bone and the host femur (Fig. 4C). Mobilization of CFU-S from ectopic bone into the peripheral blood is the most likely cause since the induction of HSCs was accompanied by dynamic osteogenesis. The increased HSC number in the host bone marrow can be explained by HSC mobilization from ectopic bone into the peripheral blood. In the normal mice, such migration or mobilization of hematopoietic cells occurs during development. Hematopoietic events in the mouse begin in the yolk sac and aorta-gonad-mesonephros region at day 7 of gestation, and

they shift the site to the fetal liver at mid-gestation followed by the bone marrow shortly before birth. The prevailing notion has been that this sequence reflects the migration of HSCs from the yolk sac to the definitive hematopoietic sites. Observation in this study, that is, the generation of ectopic bone in the subcutaneous tissues and the resultant migration of HSCs via the peripheral blood, seems to mimic above process during developments (Dzierzak et al., 1998).

Unexpected upregulation of MHC antigen after implantation of donor cells

Although most HSCs have been reported to express MHCs, that is, HLA in humans, and H-2 antigens in mice, no mesenchymal stem cells have been reported to express MHC antigens at least in vitro (Jiang et al., 2002). Since lack of these antigens on the cell surface may contribute to the induction of tolerance in these cells when transplanted in allogeneic combination, the complete rejection of the transplanted mesenchymal cells and de novo expression of the H-2 antigen after in vivo implantation was contrary to our expectation. We do not know the molecular mechanisms responsible for upregulated expression of H-2 and downregulated expression of Sca-1 after cell implantation, but care should be exercised when mesenchymal cells are implanted for therapeutic purposes, because membrane-bound molecules, including functionally essential molecules, might be modulated after implantation.

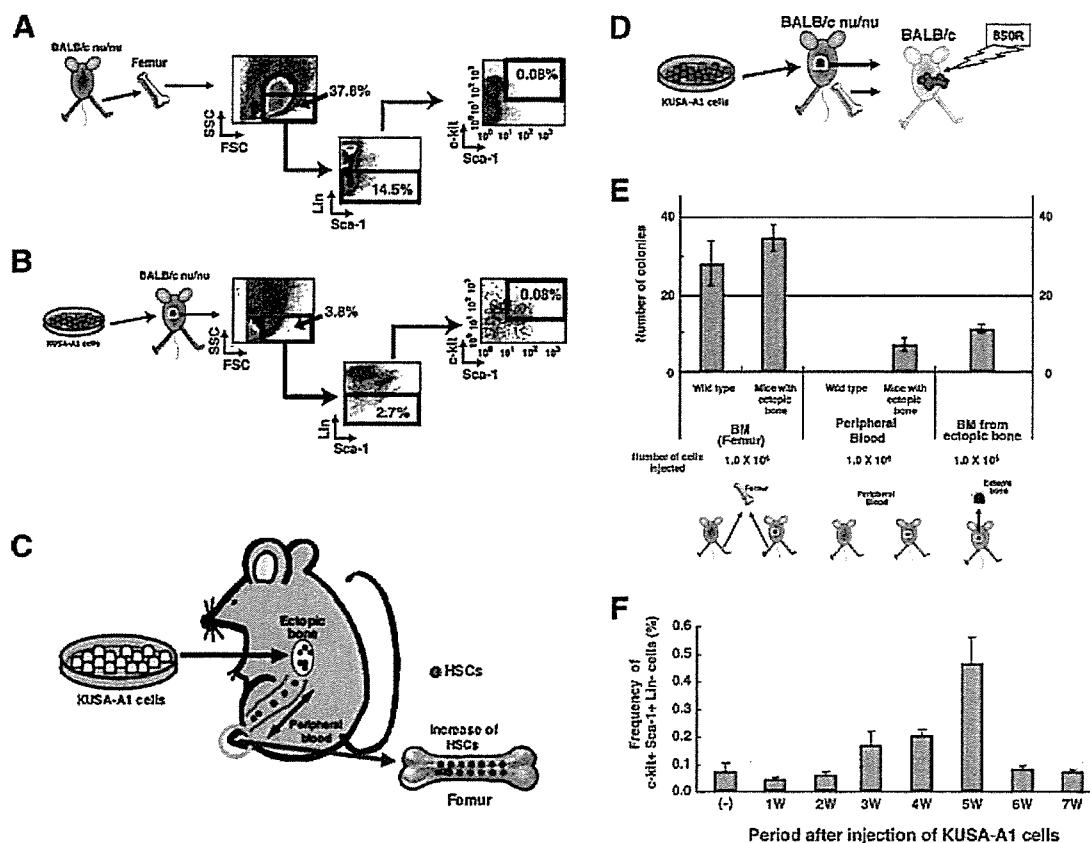


Fig. 4. Mobilization of $c\text{-kit}^+ \text{Sca-1}^+ \text{Lin}^-$ (KSL) cells in the ectopic bones generated by KUSA-A1 cells. A and B: Flow cytometric analysis of hematopoietic stem cell markers was performed on hematopoietic cells in the femur of BALB/c nu/nu mice (A) and the ectopic bone generated in BALB/c nu/nu mice (B). KSL cells accounted for 0.08% of the hematopoietic cells in KUSA-A1 bone. C: Proposed mechanism of HSC mobilization in the peripheral blood of mice with the ectopic bone, and the increased HSCs in the femur of mice implanted with osteoblasts. Osteoblastic cells whose number has been increased by local injection into the tissues support an increase in number of HSCs in both bone marrow and peripheral blood, as a result of an increase in size of the microenvironment or niche in vivo. The niche size defined by dynamic osteogenic process affects the number of stem cells. D: Experimental design to investigate mobilization of CFU-S in the peripheral blood of mice with the ectopic bone, and the proportion of KSL cells in the femur of mice implanted with KUSA-A1 cells.

Crucial role of marrow stromal subsets in HSC regulation

HSCs are a subset of bone marrow cells that are capable of self-renewal and of forming all types of blood cells. The increases in bone size generated by the spindle-shaped KUSA-A1 osteoblasts correlated with the increase in the number of HSCs. The osteoblasts and a subpopulation of the HSCs expressed N-cadherin, a cell-surface molecule that helps cells adhere to one another, and N-cadherin and -catenin may form important components of the interaction between HSCs and their niche (Zhang et al., 2003). The Notch signaling pathway is also known to regulate cell-fate decisions in many organisms (Calvi et al., 2003). Involvement of cytokine signaling in HSC regulation has been reported to be crucial to the development of blood-forming tissue in embryos. The doubling of bone size mirrored the increase in the HSC population in the mice implanted with KUSA-A1 cells.

The strategy to increase the size of the HSC population by implanting osteoblasts into the subcutaneous

Hematopoiesis was induced in the ectopic bone by KUSA-A1 cell implantation (See Fig. 3). The hematopoietic cells in the ectopic bone and the host femur were analyzed for further CFU-S analysis in mice exposed to 850 cGy irradiation. E: CFU-S assay in the marrow cells of the femur of mice not implanted with any cells; the femoral marrow cells of mice with ectopic bone; peripheral blood cells of mice not implanted with cells; peripheral blood cells of mice with ectopic bone; marrow cells in ectopic bone. The blood samples were obtained at 5 weeks after implantation. The number of HSC or CFU-s increased to $11.2 \pm 0.8/1.0 \times 10^5$ cells in the KUSA-A1-induced ectopic bone. CFU-s in the peripheral blood increased to $7.0 \pm 1.7/10^6$ cells at day 12 after implantation of the KUSA-A1 cells while no CFU-s were detected in the peripheral blood from mice without cell implantation. F: Time course of the proportion of KSL cells in the femur of mice implanted with KUSA-A1 cells.

tissue to increase the osteoblast cell population may be proven to be of certain clinical value in the future. The concept that a microenvironment or niche controls HSCs may be useful for HSC expansion in vivo, and has potential implications for HSC harvesting and recovery after transplantation (Fig. 4C). Direct implantation of KUSA-A1 cells into syngeneic or immunodeficient mice, in order to better understand the interactions between HSCs and bone marrow, may therefore lead to the development of practical methods of manipulating stem cells and define a model for investigating the impact of the microenvironment on cell physiology (Li et al., 2000). Cellular and molecular identification using the strategy of niche-constituent cells or signaling pathways will provide pharmacological targets with therapeutic potential for stem-cell-based therapies.

ACKNOWLEDGMENTS

This study was supported by a grant from the Ministry of Education, Culture, Sports, Science, and Technology (MEXT) of Japan and the Health and Labour Sciences Research Grants, and the Pharmaceuticals and Medical

Devices Agency to A. U. We thank T. Tsurumi and T. Shimizu for their excellent technical assistance in animal and cell culture.

LITERATURE CITED

- Calvi LM, Adams GB, Weibrecht KW, Weber JM, Olson DP, Knight MC, Martin RP, Schipani E, Divieti P, Bringhurst FR, Milner LA, Kronenberg HM, Scadden DT. 2003. Osteoblastic cells regulate the haematopoietic stem cell niche. *Nature* 425:841–846.
- Dzierzak E, Medvinsky A, de Bruijn M. 1998. Qualitative and quantitative aspects of haematopoietic cell development in the mammalian embryo. *Immunol Today* 19:228–236.
- Goodell MA, Brose K, Paradis G, Conner AS, Mulligan RC. 1996. Isolation and functional properties of murine hematopoietic stem cells that are replicating in vivo. *J Exp Med* 183:1797–1806.
- Harrison DE, Russell ES. 1972. The response of W-W v and Sl-Sl d anaemic mice to haemopoietic stimuli. *Br J Haematol* 22:155–168.
- Ikehara S. 2000. Pluripotent hemopoietic stem cells in mice and humans. *Proc Soc Exp Biol Med* 223:149–155.
- Jiang Y, Jahagirdar BN, Reinhardt RL, Schwartz RE, Keene CD, Ortiz-Gonzalez XR, Reyes M, Lenvik T, Lund T, Blackstad M, Du J, Aldrich S, Lisberg A, Low WC, Largaespada DA, Verfaillie CM. 2002. Pluripotency of mesenchymal stem cells derived from adult marrow. *Nature* 418:41–49.
- Kohyama J, Abe H, Shimazaki T, Koizumi A, Nakashima K, Gojo S, Taga T, Okano H, Hata J, Umezawa A. 2001. Brain from bone: Efficient “meta-differentiation” of marrow stroma-derived mature osteoblasts to neurons with Noggin or a demethylating agent. *Differentiation* 68:235–244.
- Li Y, Hisha H, Inaba M, Lian Z, Yu C, Kawamura M, Yamamoto Y, Nishio N, Toki J, Fan H, Ikehara S. 2000. Evidence for migration of donor bone marrow stromal cells into recipient thymus after bone marrow transplantation plus bone grafts: A role of stromal cells in positive selection. *Exp Hematol* 28:950–960.
- Lord BI. 1990. The architecture of bone marrow cell populations. *Int J Cell Cloning* 8:317–331.
- Makino S, Fukuda K, Miyoshi S, Konishi F, Kodama H, Pan J, Sano M, Takahashi T, Hori S, Abe H, Hata J, Umezawa A, Ogawa S. 1999. Cardiomyocytes can be generated from marrow stromal cells in vitro. *J Clin Invest* 103:697–705.
- Matsuzaki Y, Kinjo K, Mulligan RC, Okano H. 2004. Unexpectedly efficient homing capacity of purified murine hematopoietic stem cells. *Immunity* 20: 87–93.
- Mori T, Kiyono T, Imabayashi H, Takeda Y, Tsuchiya K, Miyoshi S, Makino H, Matsumoto K, Saito H, Ogawa S, Sakamoto M, Hata J-I, Umezawa A. 2005. Combination of hTERT and Bmi-1, E6 or E7 induce prolongation of the life span of bone marrow stromal cells from an elderly donor without affecting their neurogenic potential. *Mol Cell Biol* 25:5183–5195.
- Okada S, Nakauchi H, Nagayoshi K, Nishikawa S, Miura Y, Suda T. 1991. Enrichment and characterization of murine hematopoietic stem cells that express c-kit molecule. *Blood* 78:1706–1712.
- Okada S, Nakauchi H, Nagayoshi K, Nishikawa S, Miura Y, Suda T. 1992. In vivo and in vitro stem cell function of c-kit- and Sca-1-positive murine hematopoietic cells. *Blood* 80:3044–3050.
- Osawa M, Hanada K, Hamada H, Nakauchi H. 1996. Long-term lymphohematopoietic reconstitution by a single CD34-low/negative hematopoietic stem cell. *Science* 273:242–245.
- Pittenger MF, Mackay AM, Beck SC, Jaiswal RK, Douglas R, Mosca JD, Moorman MA, Simonetti DW, Craig S, Marshak DR. 1999. Multilineage potential of adult human mesenchymal stem cells. *Science* 284:143–147.
- Schöfield R. 1978. The relationship between the spleen colony-forming cell and the haemopoietic stem cell. *Blood Cells* 4:7–25.
- Sharov AA, Piao Y, Matoba R, Dudekula DB, Qian Y, VanBuren V, Falco G, Martin PR, Stagg CA, Bassey UC, Wang Y, Carter MG, Hamatani T, Aiba K, Akutsu H, Sharova L, Tanaka TS, Kimber WL, Yoshikawa T, Jaradat SA, Pantano S, Nagaraja R, Boheler KR, Taub D, Hodess RJ, Longo DL, Schlessinger D, Keller J, Klotz E, Kelsoe G, Umezawa A, Vescovi AL, Rossant J, Kunath T, Hogan BL, Curci A, D’Urso M, Kelsoe J, Hide W, Ko MS. 2003. Transcriptome analysis of mouse stem cells and early embryos. *PLoS Biol* 1:E74.
- Siminovitch L, McCulloch EA, Till JE. 1963. The distribution of colony-forming cells among spleen colonies. *J Cell Physiol* 62:327–336.
- Spangrude GJ, Heimfeld S, Weissman IL. 1988. Purification and characterization of mouse hematopoietic stem cells. *Science* 241:58–62.
- Takeda Y, Mori T, Imabayashi H, Kiyono T, Gojo S, Miyoshi S, Hida N, Ita M, Segawa K, Ogawa S, Sakamoto M, Nakamura S, Umezawa A. 2004. Can the life span of human marrow stromal cells be prolonged by bmi-1, E6, E7, and/or telomerase without affecting cardiomyogenic differentiation? *J Gene Med* 6:833–845.
- Terai M, Uyama T, Sugiki T, Li XK, Umezawa A, Kiyono T. 2005. Immortalization of human fetal cells: the life span of umbilical cord blood-derived cells can be prolonged without manipulating p16INK4a/RB braking pathway. *Mol Biol Cell* 16:1491–1499.
- Till JE, McCulloch CE. 1961. A direct measurement of the radiation sensitivity of normal mouse bone marrow cells. *Radiat Res* 14:213–222.
- Till JE, McCulloch EA, Siminovitch L. 1964. A stochastic model of stem cell proliferation, based on the growth of spleen colony-forming cells. *Proc Natl Acad Sci USA* 51:29–36.
- Umezawa A, Maruyama T, Segawa K, Shadduck RK, Waheed A, Hata J. 1992. Multipotent marrow stromal cell line is able to induce hematopoiesis in vivo. *J Cell Physiol* 151:197–205.
- Watt FM, Hogan BL. 2000. Out of Eden: Stem cells and their niches. *Science* 287:1427–1430.
- Weissman IL. 2000. Stem cells: Units of development, units of regeneration, and units in evolution. *Cell* 100:157–168.
- Yoshimoto M, Shinohara T, Heike T, Shiota M, Kanatsu-Shinohara M, Nakahata T. 2003. Direct visualization of transplanted hematopoietic cell reconstitution in intact mouse organs indicates the presence of a niche. *Exp Hematol* 31: 733–740.
- Zhang J, Niu C, Ye L, Huang H, He X, Tong WG, Ross J, Haug J, Johnson T, Feng JQ, Harris S, Wiedemann LM, Mishina Y, Li L. 2003. Identification of the haematopoietic stem cell niche and control of the niche size. *Nature* 425: 836–841.

Differentiation of Adult Stem Cells Derived from Bone Marrow Stroma into Leydig or Adrenocortical Cells

Takashi Yazawa, Tetsuya Mizutani, Kazuya Yamada, Hiroko Kawata, Toshio Sekiguchi, Miki Yoshino, Takashi Kajitani, Zhangfei Shou, Akihiro Umezawa, and Kaoru Miyamoto

Department of Biochemistry (T.Y., T.M., K.Y., H.K., T.S., M.Y., T.K., Z.S., K.M.), Faculty of Medical Sciences, University of Fukui, Fukui 910-1193, Japan; Core Research for Evolutional Science and Technology (T.Y., T.M., K.Y., H.K., T.S., M.Y., T.K., Z.S., K.M.), Japan Science and Technology Agency, Saitama 332-0012, Japan; and National Research Institute for Child Health and Development (A.U.), Tokyo 157-8535, Japan

Adult stem cells from bone marrow, referred to as mesenchymal stem cells or marrow stromal cells (MSCs), are defined as pluripotent cells and have the ability to differentiate into multiple mesodermal cells. In this study, we investigated whether MSCs from rat, mouse, and human are able to differentiate into steroidogenic cells. When transplanted into immature rat testes, adherent marrow-derived cells (including MSCs) were found to be engrafted and differentiate into steroidogenic cells that were indistinguishable from Leydig cells. Isolated murine MSCs transfected with green fluorescence protein driven by the promoter of P450 side-chain cleaving enzyme gene (CYP11A), a steroidogenic cell-specific gene, were used to detect steroidogenic cell production *in vitro*.

During *in vitro* differentiation, green fluorescence protein-positive cells, which had characteristics similar to those of Leydig cells, were found. Stable transfection of murine MSCs with a transcription factor, steroidogenic factor-1, followed by treatment with cAMP almost recapitulated the properties of Leydig cells, including the production of testosterone. Transfection of human MSCs with steroidogenic factor-1 also led to their conversion to steroidogenic cells, but they appeared to be glucocorticoid- rather than testosterone-producing cells. These results indicate that MSCs represent a useful source of stem cells for producing steroidogenic cells that may provide basis for their use in cell and gene therapy. (*Endocrinology* 147: 4104–4111, 2006)

STEM CELLS ARE self-renewing elements with the capacity to generate multiple distinct cell lineages. They exist in various tissues, even in adults, and have been isolated from a variety of differentiated tissues, including bone marrow, umbilical blood, brain, and fat (1–6). Among these, bone marrow-derived mesenchymal stem cells (MSCs), also known as marrow stromal cells, are defined as pluripotent cells and have been shown to differentiate into adipocytes, chondrocytes, osteoblasts, and hematopoietic-supporting stroma both *in vivo* and *ex vivo* (1–3). Furthermore, they are able to generate cells of all three germ layers (7, 8). In addition to their multipotency for differentiation, MSCs have attracted considerable interest for use in cell and gene therapy because these cells can easily be obtained from adult marrow tissue (8–10).

The gonad and adrenal gland are the primary steroidogenic organs in mammals. In the gonad, male Leydig cells or female granulosa and theca cells are responsible for the production of androgens and estrogens. The adrenal cortex produces glucocorticoids and mineralocorticoids, although

some androgens are also produced in many species, except rodents. These steroidogenic organs develop from the common adrenogenital primordium, which originates from the intermediate mesoderm (11). Fetal-type steroidogenic cells appear when the adrenogenital primordium differentiates into the adrenal cortex and the gonads of the two sexes. These are replaced by adult-type steroidogenic cells during the period between birth and puberty (12, 13), but these processes are poorly understood.

One approach to resolving the complexities of organogenesis is to use stem cells as a model system for differentiation. In this study, the differentiation of MSCs into steroidogenic cells was examined *in vivo* and *in vitro* by several methods. A number of studies have reported that the injection of MSCs into some tissues leads to the differentiation of the injected cells into tissue-specific cells, probably due to the microenvironment near the injection sites. To determine whether MSCs are able to differentiate into steroidogenic cells, we injected a purified population of rat MSCs into the prepubertal rat testis and examined the fate of these cells by immunohistochemistry. In addition, the spontaneous differentiation of MSCs to specific cells can be monitored by the expression of specific genes in the differentiated cells. One such experimental approach, known as a promoter-sorting method, is to use fluorescence-activated cell sorting (FACS) to select green fluorescence protein (GFP)-positive MSCs in which the expression of GFP is under the control of the promoter of a gene that is expressed in a cell type-specific fashion. In this study, to demonstrate the emergence of steroidogenic cells from isolated MSCs *in vitro*, a GFP expression vector driven by the CYP11A promoter (CYP11A is a

First Published Online May 25, 2006

Abbreviations: ES, Embryonic stem; FACS, fluorescence activated cell sorting; GFP, green fluorescence protein; hMSC, human MSC; 3β -HSD I, 3β -hydroxysteroid dehydrogenase I; 17β -HSD III, 17β -hydroxysteroid dehydrogenase III; mMSC, murine MSC; MSC, mesenchymal stem cell; P450arom, cytochrome P450 aromatase; P450c17, cytochrome P450 17α -hydroxylase; P450c21, cytochrome P450 steroid 21 -hydroxylase; P450sc, P450 side-chain cleaving enzyme; SF, steroidogenic factor; StAR, steroidogenic acute regulatory protein.

Endocrinology is published monthly by The Endocrine Society (<http://www.endo-society.org>), the foremost professional society serving the endocrine community.

gene encoding the cholesterol side-chain cleavage enzyme, an essential enzyme for steroidogenesis) was integrated into the MSCs, and GFP-positive MSCs were then separated by fluorocytometry. Finally, to achieve the efficient differentiation of the isolated MSCs *in vitro*, the orphan nuclear receptor, steroidogenic factor (SF)-1 was ectopically expressed in MSCs. MSCs successfully differentiated into steroidogenic cells using any of these procedures. These results indicate that MSCs represent a useful source of stem cells for producing steroidogenic cells that may provide basis for their use in cell and gene therapy.

Materials and Methods

Animals

GFP transgenic rats [SD TgN(act-EGFP)OsbCZ-004] were kindly provided by Dr. M. Okabe (Osaka University, Osaka, Japan). Sprague Dawley rats were purchased from Sankyo (Shizuoka, Japan). At all times, the animals were treated according to National Institutes of Health guidelines. The donor animals used in this study were generally 4–5 wk old, and the recipient animals were 3 wk old.

Histology and immunofluorescence analysis

Immunohisto- and cytochemical staining with antirat P450 side-chain cleaving enzyme (P450scc) (C-16; Santa Cruz Biotechnology, Santa Cruz, CA), antimouse 3 β -hydroxysteroid dehydrogenase I (3 β -HSD I) (kindly provided by Dr. A. Payne, Stanford University Medical Center, Stanford, CA), antipig cytochrome P450 17 α -hydroxylase (P450c17) (kindly provided by Dr. D. Hales, University of Illinois at Chicago, Chicago, IL) or anti-GFP (Medical & Biological Laboratories Co., Ltd.) were performed on 10- μ m frozen sections or cultured cells on glass slides using standard protocols. Appropriate Cy3- or fluorescein isothiocyanate-conjugated secondary antibodies (Sigma, St. Louis, MO) were used for detection.

Cell culture, stable transfection, and hormone assay

MSCs from GFP transgenic rats were collected and cultured as described by Pochampally *et al.* (14). Mouse (KUM9) (15) or human (hMSC-hTERT-E6/E7) (16) bone marrow-derived MSCs were maintained in Iscova's MEM or DMEM with 10% fetal calf serum. Plasmid DNA was transfected using the LipofectAmine PLUS reagent (Invitrogen, Carlsbad, CA) or calcium phosphate coprecipitation. Cells were used for the experiments after 10–12 passages, and steroid hormone production was sustained for at least 4 months. The levels of each steroid hormone in the media were measured by RIA.

Transplantation

Bone marrow cells from TgN(ActbEGFP) transgenic rats (1×10^6) were injected into the testes of 3-wk-old SD rats. Two to three weeks after transplantation, testes were removed to examine histochemically survival and differentiation of transplanted cells.

Plasmid construction

A 2.3-kb fragment of the human CYP11A (P450scc gene) promoter that functions specifically in steroidogenic organs (17) was obtained by PCR using pSCC2300-LacZ (kindly provided by Dr. B. C. Chung, Institute of Molecular Biology, Taipei, Taiwan) as a template and integrated into a promoter-less pEGFP-1 vector (CLONTECH, Palo Alto, CA). The *EcoRI*-*StuI* restriction fragment, containing the CYP11A promoter-GFP, was then excised and inserted into *EcoRI* and *SmaI* site of pPUR (CLONTECH). The expression vector for rat SF-1 cDNA containing the entire coding region was generated by RT-PCR and subcloned into pIRES-puro2 vector (CLONTECH).

FACS analysis and cell purification

Cells were harvested by treatment with 0.25% trypsin/EDTA, after which they were neutralized with DMEM with 10% fetal calf serum,

washed twice with PBS, and filtered through a 35-mm pore size nylon screen. FACS analysis was performed on a flow cytometer with a 488-nm argon laser and GFP-positive cells were isolated.

RT-PCR and real-time PCR

Total RNA from the cultured cells was extracted using the Trizol reagent (Invitrogen). RT-PCR was performed as described previously (18). The reaction mixture was subjected to electrophoresis in a 1.5% agarose gel, and the resulting bands were visualized by staining with ethidium bromide. Real-time PCR was performed as described by Rutledge and Cote (19). Reagents for real-time PCR were purchased from Applied Biosystems (Warrington, UK), except for SYBER green PCR master mix (QIAGEN, Valencia, CA). Reactions were carried out and fluorescence was detected on a GeneAmp 7700 system (Applied Biosystems). The primers used are shown in Table 1.

Western blot analysis

The extraction of protein from the cultured cells and subsequent quantification was performed as described previously (20). Equal amounts of protein (50 μ g) were resolved by 12.5% SDS-PAGE and transferred to polyvinylidene difluoride membranes. Western blot analyses of SF-1, steroidogenic acute regulatory protein (StAR), P450scc, 3 β -HSD I, P450c17, and β -tubulin were carried out with antisera directed against SF-1 (Ad4BP, kindly provided by Dr. K. Morohashi, National Institute of Basic Biology, Okazaki, Japan), StAR (kindly provided by Dr. W. Miller, University of California, San Francisco, CA) (21), P450scc (kindly provided by Dr. B. C. Chung) (22), 3 β -HSD I (kindly provided by Dr. A. Payne), P450c17 (kindly provided by Dr. D. Hales) (23), and β -tubulin (D-10, Santa Cruz). ECL Western blot reagents (Amersham Pharmacia Biotech, Piscataway, NJ) were used for detection.

Results

Transplantation of rat bone marrow mesenchymal stem cells

In the prepubertal testis, fetal-type Leydig cells are replaced by adult-type Leydig cells, which originate from mesenchymal precursor cells that are present in the testicular interstitium (12). To determine whether MSCs can be engrafted into the testis and converted into steroidogenic cells we took 1×10^6 bone marrow cells from TgN(ActbEGFP) transgenic rats that had been maintained in culture (Fig. 1A) and injected them into the testes of 3-wk-old SD rats. As shown in Fig. 1C, donor engraftment was confirmed (100%) at various periods after transplantation (1–4 wk). A histochemical examination revealed that the GFP-positive cells present in the testes were located in the interstitium and were not observed within the seminiferous tubules (Fig. 1D). An immunohistochemical study showed that most of the GFP-positive cells in the interstitium were also positive for three Leydig cell markers, P450scc (Fig. 1E), 3 β -HSD I, and P450c17 (data not shown). These results indicate that donor derived-plastic adhered marrow cells had in fact differentiated into steroidogenic Leydig-like cells *in vivo*.

Gene promoter sorting

Although these data suggest that the injected stem cells differentiated into Leydig cells, the apparent stem cell plasticity may also be explained by possible cell-nuclear fusion between donor and recipient cells, as has been recently suggested (24). Therefore, we next performed *in vitro* experiments to determine whether purified murine MSCs (mMSCs), KUM9 (15), have the capacity to differentiate into steroidogenic cells. To detect a cell population committed to

TABLE 1. Primers for RT-PCR and real-time PCR

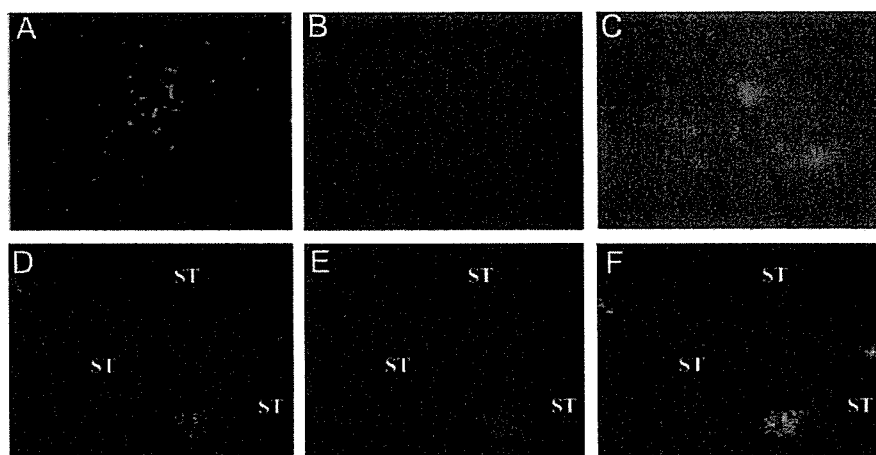
Gene	Sequence	Gene	Sequence
RT-PCR		RT-PCR	
SF-1	F-CGCACAGTCCAGAACAACAAGCA R-CGGTTAGAGAAGGCAGGATAGAG	hHSD3b2	F-CAGTGTGCCAGTCTTCATCT R-AGCAGGAAGCCAATCCAGTA
mStAR	F-GAAGGAAAGCCAGCAGGAGAACG R-CTCTGATGACACCACTCTGCTCC	hP450c17	F-CATGCTGGACACACTGATGC R-GGTGTATCTCTAAAAATCTGT
mP450scc	F-TTCCGCTTTTCCTTTGAGTCCAT R-GTGTCTCCTTGATGCTGGCTTTT	hHSD17b3	F-GCAGATTTTACAAAAGATGACAT R-TCATGGGCAAGGCAGCCACAGGT
mHSD3b1	F-ACTGCAGGAGGTGACAGCT R-GCCAGTAACACAGAATACC	hP450c21	F-TGCCTGCCTATTACAAATGT R-GGTGAAGCAAAAAACCACG
mHSD3b6	F-TCTGGAGGAGATCAGGGTC R-GCCCGTACAACCGAGAATATT	hP45011 b1	F-ACATTGGTGCGCGTGTTCCTC R-GAGACGTGATTAGTTGATGGC
mP450c17	F-AAATAATAACACTGGGGAAGGC R-TGGGTGTGGGTGTAATGAGATGG	hP450 11b2	F-TACAGGTTTTCTCTACTCG R-AGATGCAAGACTAGTTAATC
mP450c21	F-AGAGGATCCGCTTGGGGCTGC R-GGAGGAATTCCTTATGGATGGC	hP450aro	F-CTGGAAGAATGTATGGACTT R-GATCATTTCCAGCATGTTTT
mP450 11b1	F-TCACCAATGTATCAAGAATGTGT R-CCATCTGCACATCTCTTTCTCTT	β -Actin	F-GGGAATCGTGGTGACATTAAG R-TGTGTTGGCGTACAGGCTTTG
mP450 11b2	F-CCAACAGATGTATCTGGAAGGTGC R-CCATCTGCACATCTCTTGCCCTCA	hIGF-2	F-AGTCGATGCTGGTGCTTCTACCTCTT R-TGCCGCGATTTTGCTCACTTCCGATT
mLHR	F-CTCCACCTATCTCCCTGTC R-TCTTTCTTCGGCAAATTCCTG	Real-time PCR	
mACTHR	F-GCTCCAAGGATCATTTACTTGC R-CGCCAGGAGGCTTAACATAAC	mP450scc	F-CCAGTGTCCCATGCTCAAC R-TGCATGTCCTTCCAGGTCT
GAPDH	F-ACCACAGTCCATGCCATCAC R-TCCACCACCCTGTTGCTGA	mHSD3b1	F-TAACAAATTTAACAGCCCCCTCCTAAGG R-ATCCAGCCATGGTCAACACA
GFP	F-TGACCACCCTGACCTACGGCGT R-GGTAGTGGTTGTTCGGGCAGCA	mHSD3b6	F-AAACCATCCTCCACTGTTCTAGCT R-TGGAGATGGTCAGCCACAAG
mHSD17b3	F-ATTTTACCAGACAAGACATCT R-GGGGTCAGCACCTGAATAATG	mP450c17	F-AGTTTGCCATCCCGAAGGA R-CTGGCTGGTCCATTCAATTT
mP450aro	F-TCAATACCAGGTCTCGGCTA R-GTATGCACTGATTACAGTTC	mHSD17b3	F-TGGGACAATGGGCAGTGAT R-GCCAACTCAAATGAATAGGCTTTC
hStAR	F-GAGAGTCAGCAGGACAATGG R-CTGGTTGATGATGCTCTTGG	β -Actin	F-CAACCGTGAAAAGATGACCCAGATC R-AGTCCATCACAATGCCTGTGGTAC
hP450scc	F-TAGTGTCTCCTTGATGCTGG R-GAAAGGAAGTGTTCACCACG		

F, Forward; R, reverse.

the steroidogenic lineage, we first introduced a human CYP11A1 promoter/GFP gene construct into the mMSCs. This was accomplished by using a 2.3-kb fragment of the promoter region of the human CYP11A1 (a gene that encodes cytochrome P450scc, cholesterol side-chain cleavage enzyme), which has been shown to selectively drive transgene expression to adrenal and gonadal steroidogenic cells (17). In some of the transformed cell lines, GFP fluorescence was detected, as shown in Fig. 2, B and C, but the number of GFP-expressing cells was very low. Thus, GFP-positive cells were enriched by sorting with flow cytometry (Fig. 2E, 1–5% of total cells). As shown in Fig. 2, F and G, enriched GFP-

positive cells were also positive for P450scc, indicating that a very small but distinct portion of the mMSCs had spontaneously differentiated into cells that produce the steroid hormone-synthesizing enzyme. Further analysis of the differentiated cells revealed the expression of several genes that are specific to testicular Leydig cells, as shown in Fig. 2H. These include a nuclear orphan receptor SF-1, 3 β -HSD types I and VI, and LH receptor (Fig. 2H, lane SCC+). LH receptor and 3 β -HSD VI are known to be typical markers for androgen producing cells, such as Leydig cells (25). These observations further support the *in vivo* findings that rodent MSCs have the capacity to differentiate into Leydig-like cells in the testis.

FIG. 1. Transplantation of GFP-positive MSCs into the testis. A, Fluorescence view of MSCs from a green rat 3 d after the first passage. Fluorescence microscopic view of testis before (B) or 3 wk after (C) MSC transplantation. Double staining of frozen sections from the testis 5 wk after MSC transplantation with anti-GFP (D) and anti-P450_{scc} (E) antibodies. F, Merged fluorescent image of D and E. ST, Seminiferous tubule.



Stable transfection of SF-1 into mouse MSCs

It is noteworthy that SF-1 expression was induced in the GFP-positive cells (Fig. 2H). SF-1, also known as Ad4BP, regulates the cell-specific expression of a variety of proteins that are involved in steroidogenesis, in addition to its roles in reproduction and gonadal differentiation (26). Therefore,

we next examined the effects of the stable transfection of SF-1 to mMSCs. Various cell lines that stably express SF-1 were isolated. As shown in Fig. 3C, SF-1-induced morphological changes in the cells, such as the accumulation of numerous lipid droplets. However, the transformed cells did not express steroidogenic enzyme genes or produce any steroid

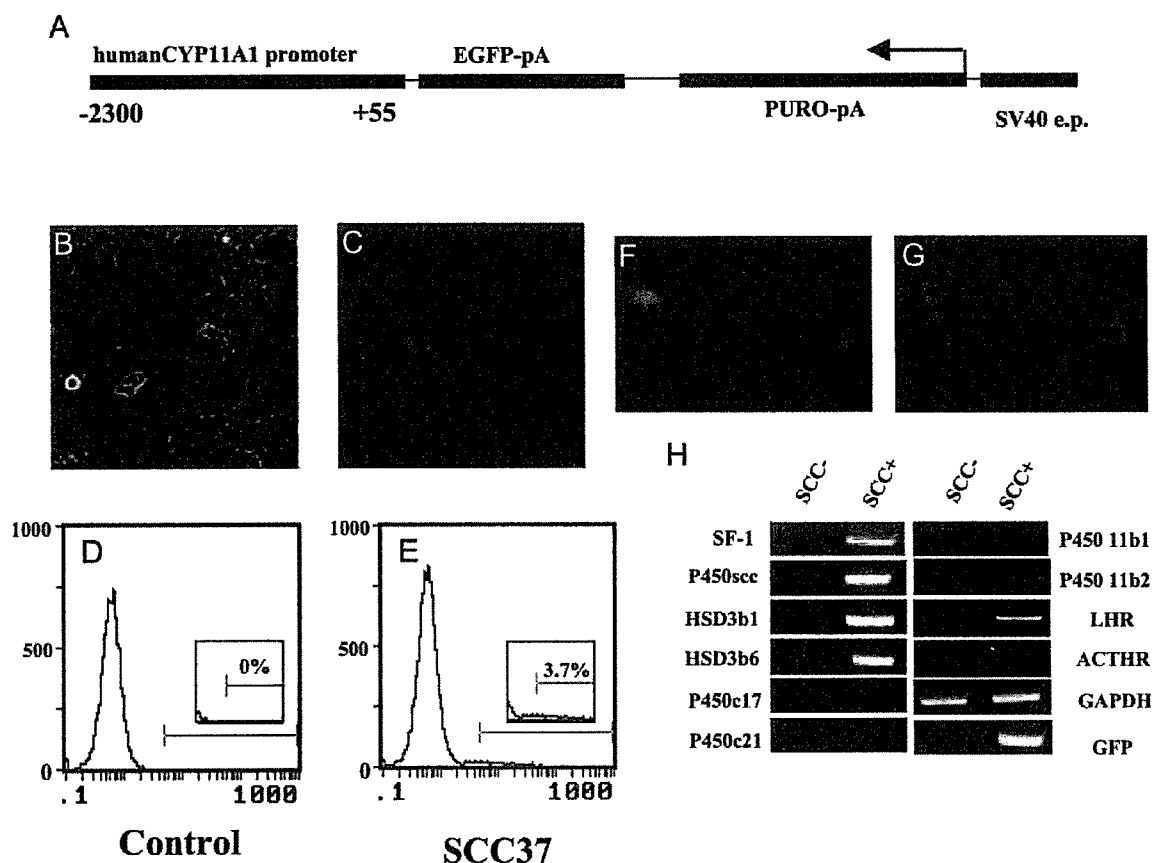


FIG. 2. Spontaneous differentiation of KUM9 into steroidogenic cells. A, Schematic representation of the SCC-reporter gene (SCC-GFP). The SCC-GFP reporter plasmid contains the 2300-bp upstream sequence of the human CYP11A1 gene and the puromycin-*N*-acetyltransferase gene (PURO-pA) driven by the Simian virus 40 early promoter (SV40 e.p.). Phase-contrast (B) and fluorescent (C) images of mMSCs transfected with SCC-GFP and selected by puromycin are shown. Flow cytometric analysis of enhanced GFP (EGFP) expression in KUM9 transfected with control-GFP (D) or SCC-GFP (E) are shown. KUM9-derived cells expressing GFP (F) under the control of the human CYP11A1 promoter were immunocytochemically stained with anti-P450_{scc} antibody (G). H, SCC-GFP-positive (SCC+) and negative (SCC-) populations were sorted and analyzed for various marker genes by RT-PCR.

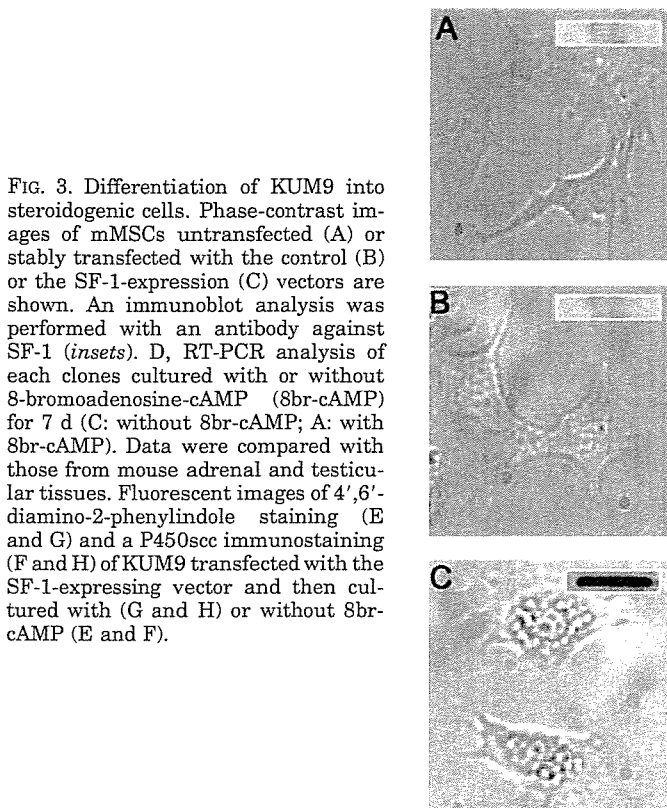
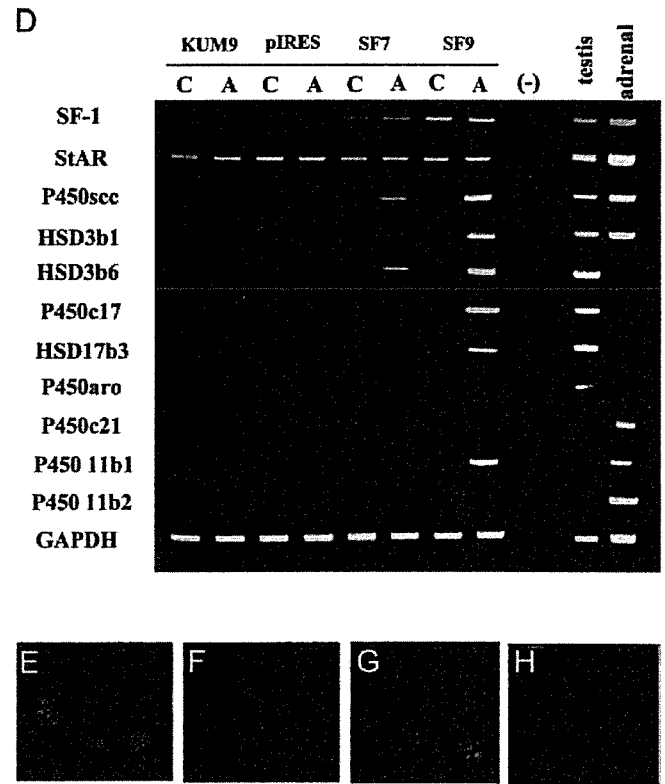


FIG. 3. Differentiation of KUM9 into steroidogenic cells. Phase-contrast images of mMSCs untransfected (A) or stably transfected with the control (B) or the SF-1-expression (C) vectors are shown. An immunoblot analysis was performed with an antibody against SF-1 (insets). D, RT-PCR analysis of each clones cultured with or without 8-bromoadenosine-cAMP (8br-cAMP) for 7 d (C: without 8br-cAMP; A: with 8br-cAMP). Data were compared with those from mouse adrenal and testicular tissues. Fluorescent images of 4',6'-diamino-2-phenylindole staining (E and G) and a P450scc immunostaining (F and H) of KUM9 transfected with the SF-1-expressing vector and then cultured with (G and H) or without 8br-cAMP (E and F).



hormones (Fig. 3D and Table 2). Therefore, we next added cAMP to the cultures because cAMP is known to induce steroidogenesis in a number of steroidogenic cell lines. Treatment of confluent cultures with cAMP was found to induce both P450scc mRNA (Fig. 3D) and protein (Fig. 3H) in the transformed cell lines, SF7 and SF9, whereas no induction was observed in untransfected (KUM9) or vector-transfected (pIRES) mMSCs (Fig. 3D). Treatment of the cells for a period of 7 d further induced the expression of other steroidogenic enzyme genes, as shown in Fig. 3D. Several cell lines showed similar expression patterns (two of which are shown in Fig. 3D).

3 β -HSD types I and VI were induced 3 d after cAMP treatment (Fig. 4). In the testis, the formation of testosterone is dependent on 3 β -HSD activity, and isoform types I and VI have been shown to be expressed in the adult mouse testis (27). P450c17 and 17 β -hydroxysteroid dehydrogenase III

(17 β -HSD III) were induced 5 d after the treatment (Fig. 4). It is interesting to note that the order of induction of the enzymes is similar to the sequential order for the steroid hormone synthetic pathway. 3 β -HSD enzymes are essential for the production of progesterone, and P450c17 and 17 β -HSD III are both required for the production of testosterone in testicular Leydig cells. Consistent with the expression pattern of the steroidogenic enzymes, testosterone was the major sex steroid hormone produced in the transformed cell line, SF9, when treated with cAMP for 7 d (Table 2). Two adrenal-specific steroid hormones, glucocorticoids and mineralocorticoids, were not detected in these cells. These results clearly demonstrate that the stable expression of SF-1 and the addition of cAMP induced the differentiation of mMSCs into steroidogenic cells and that these cells have properties that are similar to those of testicular Leydig cells.

TABLE 2. Production of steroid hormones by MSCs stably expressing SF-1 (SF9-KUM9 or SF4-hMSC) in the presence (+) or absence (-) of 8br-cAMP (ng/ml)

Cell (cAMP)	Progesterone	Testosterone	Estradiol	Glucocorticoid	Aldosterone
pIRES-KUM9 (-)	N.D.	N.D.	N.D.	N.D.	N.D.
pIRES-KUM9 (+)	N.D.	N.D.	N.D.	N.D.	N.D.
SF9-KUM9 (-)	N.D.	N.D.	N.D.	N.D.	N.D.
SF9-KUM9 (+)	24.3 \pm 4.25	1.6 \pm 0.29	N.D.	N.D.	N.D.
pIRES-hMSC (-)	N.D.	N.D.	N.D.	N.D.	N.D.
pIRES-hMSC (+)	N.D.	N.D.	N.D.	N.D.	N.D.
SF4-hMSC (-)	N.D.	N.D.	N.D.	N.D.	N.D.
SF4-hMSC (+)	270 \pm 82.5	17.5 \pm 0.20	0.21 \pm 0.11	520 \pm 200	1.56 \pm 0.42

Data are means and SEM values of at least duplicate assays. N.D., No detectable values.

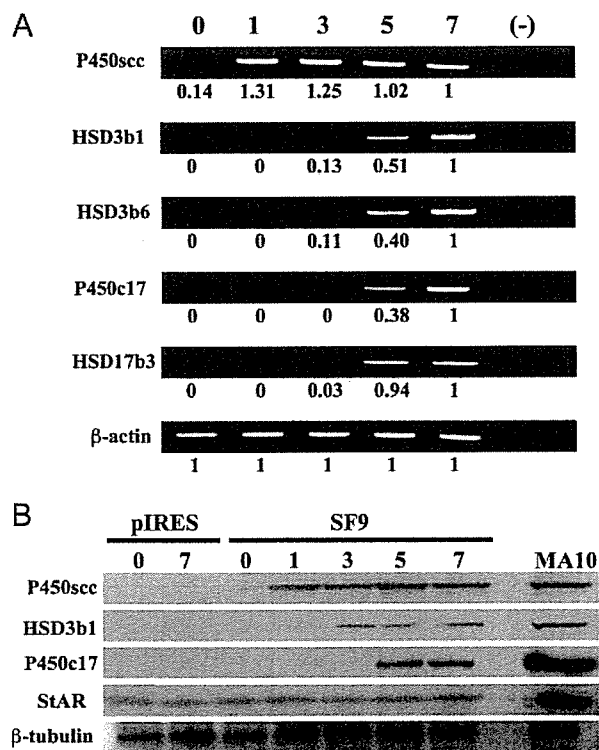


FIG. 4. Time-dependent induction of steroidogenic enzymes by cAMP. KUM9 cells stably transfected with SF-1-expression (SF9) or control (pIRES) vector were cultured and treated with 8-bromoadenosine-cAMP for the indicated times. A, P450scc, 3 β -HSD I, 3 β -HSD VI, P450c17, and 17 β -HSD III mRNA levels were analyzed by RT-PCR and real-time PCR. Real-time PCR data are the mean values of at least triplicate assays. The 7-d value was arbitrarily taken as 1.0. B, Immunoblot analyses were performed with antibodies against StAR, P450scc, 3 β -HSD I, P450c17, and β -tubulin using the same lysates. The data were compared with that from MA-10 cells treated with cAMP (4 h).

Stable transfection of SF-1 into human MSCs

We next examined the issue of whether the same approach could also be used to induce the differentiation of human MSCs (hMSCs) into steroidogenic cells. Similar to the results obtained with mMSCs, hMSCs (hMSC-TERT-E6/E7) expressed no steroidogenic enzymes or StAR before transfection with SF-1 even after cAMP treatment (Fig. 5). After SF-1 transfection, all the transformed cell lines became positive for StAR gene expression, and the expression levels were further increased by cAMP treatment. Most of the steroidogenic enzymes, P450scc, 3 β -HSD II, P450c17, cytochrome P450 steroid 21-hydroxylase (P450c21), cytochrome P450 aromatase (P450aro), and cytochrome P450 steroid 11 β -hydroxylase, were also substantially induced by cAMP stimulation. A significant difference between mMSCs and hMSCs was the strong expression of the P450c21 gene in the case of hMSCs. This caused a difference in the kinds of steroids produced by mMSCs and hMSCs. As listed in Table 2, glucocorticoids were the major steroids produced by the transformed hMSCs, hSF4, whereas testosterone was the major product from the transformed mMSCs, mSF9. The hSF4 cells mainly produced cortisol, the major glucocorticoid produced by the human adrenal gland. These results clearly demonstrate that the stable expression of SF-1 and subsequent cAMP treat-

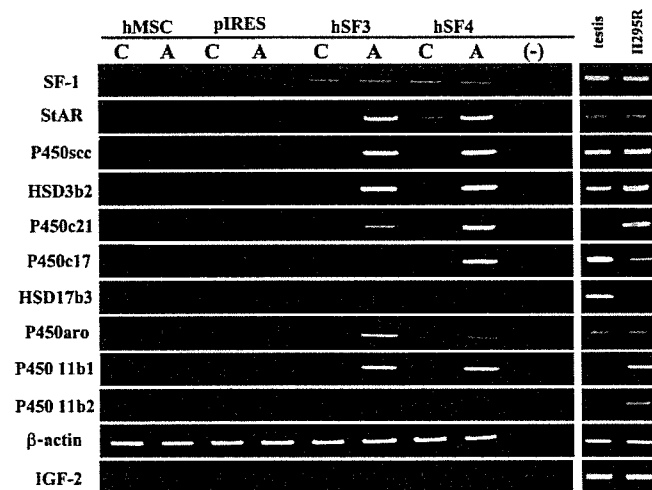


FIG. 5. Induction of steroidogenic enzymes in hMSCs. hMSCs were stably transfected with the control (pIRES) or SF-1-expression (SF3, -4) vector. RT-PCR analysis of each clone was cultured with or without 8-bromoadenosine-cAMP (8br-cAMP) for 7 d (C: without 8br-cAMP; A: with 8br-cAMP). The data were compared with that from human testis and NCI-H295R, a human adrenocortical tumor cell line, treated with cAMP (24 h).

ment induced the differentiation of hMSCs into steroidogenic cells. In addition, the cortisol-producing cells also expressed ACTH receptors and can respond to ACTH for the quick production of cortisol at nanomolar levels (data not shown).

Human MSCs also expressed P450aro as in the case of the human adrenocortical carcinoma NCI-H295R cell line (Fig. 5), whereas normal adrenal cells do not express it (28). However, hSF3 or -4 did not express IGF-II, an adrenocortical tumor marker. It has recently been shown that P450aro is expressed in human bone marrow stroma cells under certain conditions (29). Thus, it is probable that the expression of P450aro in hMSCs was not the result of a malignant phenotype or the differentiation of the cells by SF-1 and cAMP treatment.

Stable transfection of SF-1 into cells other than MSCs

We next examined the effects of transfection of SF-1 into several cell lines other than MSCs, *i.e.* a human cell line HEK293, murine embryonic stem cells, and murine cell lines F9 and NIH3T3. None of the transfected cell lines autonomously produced steroid hormones, although some were induced to express the P450scc and 3 β -HSD genes (Fig. 6).

Discussion

The findings presented herein demonstrate that rodent MSCs have the potential to differentiate into steroidogenic cells with characteristics that are very similar to testicular Leydig cells. It has been postulated that mesenchymal progenitors of Leydig cells are present in the testicular interstitium (12). Immature Leydig cells are gradually replaced by mature Leydig cells that are thought to differentiate from these mesenchymal progenitors during the prepubertal period. In fact, the injection of MSCs into the testis during this critical period caused the differentiation of MSCs into steroidogenic cells that were indistinguishable from Leydig cells. Concerning the *in vivo* experiments, the possibility of

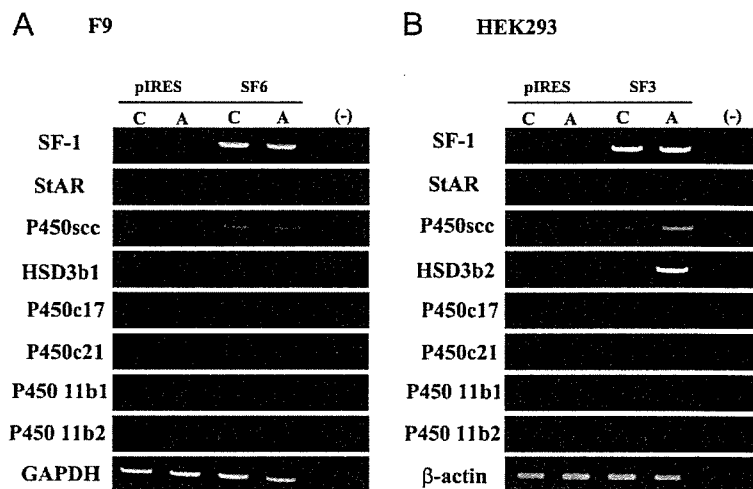


FIG. 6. Stable transfection of SF-1 and cAMP treatment for F9 (A) and HEK293 cells (B). RT-PCR analysis of steroidogenesis-related genes in each stable cell line transfected with SF-1 or pIRES (control) cultured with or without 8-bromoadenosine-cAMP (8br-cAMP) for 7 d (C: without 8br-cAMP; A: with 8br-cAMP).

cell fusion between donor MSCs and recipient testicular Leydig cells or their progenitor cells cannot be excluded. However, it should be emphasized that very small but distinct portions of mMSCs underwent spontaneous differentiation into Leydig-like cells *in vitro*. Lo *et al.* (30) demonstrated, by means of a cell transplantation assay, the presence of stem cells or progenitors for Leydig cells. Therefore, our data strongly suggest that bone marrow-derived MSCs share common properties with testicular MSCs or Leydig cell progenitors. Conversely, testicular MSCs or Leydig cell progenitors might also have pluripotent characteristics, similar to bone marrow-derived MSCs, as has been reported for some other MSCs (4, 31).

In addition, transfection of cultured mMSCs with SF-1 followed by cAMP stimulation resulted in their differentiation into Leydig cells. The same procedure also led to the successful induction of hMSCs into steroidogenic cells. In this case, however, most of the cell lines expressing SF-1 largely produced glucocorticoids rather than testosterone. This was mainly due to the strong induction of P450c21 gene expression in the hMSCs. To investigate the issue of whether hMSCs are able to differentiate into Leydig cells, we also injected hMSCs to the testis of nude mice or rats (data not shown). Unfortunately, the human cells did not survive for more than several weeks in the rodent testis.

Because the established cell lines need much longer times than general steroidogenic cells to produce steroid hormones by cAMP stimulation in this study, we speculate that cAMP treatment of this study is necessary for the induction of the cellular differentiation rather than direct stimulation of gene transcription of steroidogenic enzymes.

In hMSCs, the stable expression of SF-1 and cAMP treatment induced the expression of the StAR gene, which is essential for the transfer of cholesterol from the outer to the inner membrane of mitochondria in which the conversion of cholesterol to steroid hormones begins (21). The same treatment failed to induce StAR gene expression in several cell lines (other than MSCs) including embryonic stem (ES) cells and therefore failed to induce any steroid hormones. The expression of the P450scc or β -HSD gene was induced at low levels in some of them, however (Fig. 6). It has been reported that the stable transfection of SF-1 into ES cells

results in morphological changes and the induction of P450scc enzyme expression, (32). No autonomous production of steroid hormones was observed, however, probably because of the deficiency of cholesterol storage and mobilization and the lack of StAR protein expression (32). Therefore, our present observations suggest that MSCs, but not ES cells, are excellent precursors of steroidogenic cells. In contrast to human cells, StAR was constitutively expressed in KUM9 as well as the freshly isolated rat MSCs (our unpublished data). Therefore, we speculate that StAR gene expression is not always under the control of SF-1, and the pattern of expression may be different between species, even in the same tissues. In addition to the steroidogenesis, the movement of cholesterol to the inner mitochondrial membrane is also important for its metabolism, because one of the rate-determining steps, the 27-hydroxylation of cholesterol, is catalyzed by sterol 27-hydroxylase, which is located in the inner mitochondrial membrane (33, 34). Cholesterol metabolites, such as oxysterols have been proposed to be potential regulators of genes in cholesterol homeostasis (33). We found that sterol 27-hydroxylase mRNA was detectable in rat and mouse MSCs (data not shown), suggesting that it is involved in cholesterol metabolism. Therefore, it is assumed that the StAR protein in KUM9 is present to promote the cholesterol metabolism, despite the fact that steroidogenesis does not take place. In support of this hypothesis, ectopic expression of the StAR protein increases the metabolism of cholesterol in rat primary hepatocytes (34).

Gondo *et al.* (35) recently reported that the adenovirus-mediated forced expression of SF-1 transforms primary long-term cultured murine bone marrow cells into ACTH-responsive steroidogenic cells. In contrast to our observation obtained from murine MSCs, their steroidogenic cells produce both gonadal and adrenal steroids. There are two possible explanations for their results: 1) their cells were a mixed adrenal/gonadal phenotype or 2) were a mixture of adrenal or gonadal phenotypic cells. The latter seems to be more likely because our study clearly demonstrated the differentiation of adult stem cells derived from both murine and human into gonadal or adrenal steroidogenic cells. Therefore, with respect to the difference between mouse and human cells, we assume that the mouse MSCs used in our study were already committed to the gonadal lineage, whereas the hMSCs were already committed to

the adrenal lineage. In support of this hypothesis, it has frequently been reported that MSCs are heterogeneous populations that have a different differentiation potential (1, 2, 10). In a future study, the same treatment of various mouse or human MSCs need to be carried out, followed by observations of whether both adrenal and gonadal phenotypes are obtained. This might also provide a tool for revealing the pathway leading to the differentiation of the cells into adrenal or gonadal steroidogenic cells.

In summary, we demonstrate here that MSCs have the capacity to differentiate into steroidogenic cells, both *in vivo* and *in vitro*. MSCs represent not only a powerful tool for studies of the differentiation of the steroidogenic lineage but may also offer a possible clinical stem cell resource for diseases of steroidogenic organs.

Acknowledgments

We are grateful to Drs. K. Morohashi, W. Miller, B. C. Chung, A. Payne, and D. Hales for providing plasmids and antisera. We also thank Drs. M. Ascoli and J. Toguchida for the generous gifts of MA10 and hMSCs and Ms. Y. Inoue, T. Satake, and K. Matsuura for technical assistance.

Received February 8, 2006. Accepted May 16, 2006.

Address all correspondence and requests for reprints to: Kaoru Miyamoto, Department of Biochemistry, Faculty of Medical Sciences, University of Fukui, Shimoaizuki, Matsuoka-cho, Fukui 910-1193, Japan. E-mail: kmiyamoto@fmsrsa.fukui-med.ac.jp.

This work was supported in part by a grant from the Smoking Research Foundation and the 21st Century Center of Excellence Program (Medical Science).

All authors (T.Y., T.M., K.Y., H.K., T.S., M.Y., T.K., Z.S., A.U., K.M.) have nothing to declare.

References

- Friedenstein AJ, Gorskaja JF, Kulagina NN 1976 Fibroblast precursors in normal and irradiated mouse hematopoietic organs. *Exp Hematol* 4:267–274
- Prockop DJ 1997 Marrow stromal cells as stem cells for nonhematopoietic tissues. *Science* 276:71–74
- Ferrari G, Cusella-De Angelis G, Coletta M, Paolucci E, Stornaiuolo A, Cossu G, Mavilio F 1998 Muscle regeneration by bone marrow-derived myogenic progenitors. *Science* 279:1528–1530
- Lee OK, Kuo TK, Chen WM, Lee KD, Hsieh SL, Chen TH 2004 Isolation of multipotent mesenchymal stem cells from umbilical cord blood. *Blood* 103:1669–1675
- D'Amour KA, Gage FH 2003 Genetic and functional differences between multipotent neural and pluripotent embryonic stem cells. *Proc Natl Acad Sci USA* 100(Suppl 1):11866–11872
- De Ugarte DA, Morizono K, Elbarbary A, Alfonso Z, Zuk PA, Zhu M, Dragoo JL, Ashjian P, Thomas B, Benhaim P, Chen I, Fraser J, Hedrick MH 2003 Comparison of multi-lineage cells from human adipose tissue and bone marrow. *Cells Tissues Organs* 174:101–109
- Kopen GC, Prockop DJ, Phinney DG 1999 Marrow stromal cells migrate throughout forebrain and cerebellum, and they differentiate into astrocytes after injection into neonatal mouse brains. *Proc Natl Acad Sci USA* 96:10711–10716
- Ortiz LA, Gambelli F, McBride C, Gaupp D, Baddoo M, Kaminski N, Phinney DG 2003 Mesenchymal stem cell engraftment in lung is enhanced in response to bleomycin exposure and ameliorates its fibrotic effects. *Proc Natl Acad Sci USA* 100:8407–8411
- Chamberlain JR, Schwarze U, Wang PR, Hirata RK, Hankenson KD, Pace JM, Underwood RA, Song KM, Sussman M, Byers PH, Russell DW 2004 Gene targeting in stem cells from individuals with osteogenesis imperfecta. *Science* 303:1198–1201
- Prockop DJ, Gregory CA, Spees JL 2003 One strategy for cell and gene therapy: harnessing the power of adult stem cells to repair tissues. *Proc Natl Acad Sci USA* 100(Suppl 1):11917–11923
- Hatano O, Takakusu A, Nomura M, Morohashi K 1996 Identical origin of adrenal cortex and gonad revealed by expression profiles of Ad4BP/SF-1. *Genes Cells* 1:663–671
- Roosen-Runge EC, Anderson D 1959 The development of the interstitial cells in the testis of the albino rat. *Acta Anat (Basel)* 37:125–137
- Holmes PV, Dickson AD 1971 X-zone degeneration in the adrenal glands of adult and immature female mice. *J Anat* 108:159–168
- Pochampally RR, Neville BT, Schwarz EJ, Li MM, Prockop DJ 2004 Rat adult stem cells (marrow stromal cells) engraft and differentiate in chick embryos without evidence of cell fusion. *Proc Natl Acad Sci USA* 101:9282–9285
- Makino S, Fukuda K, Miyoshi S, Konishi F, Kodama H, Pan J, Sano M, Takahashi T, Hori S, Abe H, Hata J, Umezawa A, Ogawa S 1999 Cardiomyocytes can be generated from marrow stromal cells *in vitro*. *J Clin Invest* 103:697–705
- Okamoto T, Aoyama T, Nakayama T, Nakamata T, Hosaka T, Nishijo K, Nakamura T, Kiyono T, Toguchida J 2002 Clonal heterogeneity in differentiation potential of immortalized human mesenchymal stem cells. *Biochem Biophys Res Commun* 295:354–361
- Hu MC, Chou SJ, Huang YY, Hsu NC, Li H, Chung BC 1999 Tissue-specific, hormonal, and developmental regulation of SCC-LacZ expression in transgenic mice leads to adrenocortical zone characterization. *Endocrinology* 140:5609–5618
- Mizutani T, Yamada K, Yazawa T, Okada T, Minegishi T, Miyamoto K 2001 Cloning and characterization of gonadotropin-inducible ovarian transcription factors (GIOT1 and -2) that are novel members of the (Cys)(2)-(His)(2)-type zinc finger protein family. *Mol Endocrinol* 15:1693–1705
- Rutledge RG, Cote C 2003 Mathematics of quantitative kinetic PCR and the application of standard curves. *Nucleic Acids Res* 31:e93
- Yazawa T, Mizutani T, Yamada K, Kawata H, Sekiguchi T, Yoshino M, Kajitani T, Shou Z, Miyamoto K 2003 Involvement of cyclic adenosine 5'-monophosphate response element-binding protein, steroidogenic factor 1, and Dax-1 in the regulation of gonadotropin-inducible ovarian transcription factor 1 gene expression by follicle-stimulating hormone in ovarian granulosa cells. *Endocrinology* 144:1920–1930
- Bose HS, Whittall RM, Baldwin MA, Miller WL 1999 The active form of the steroidogenic acute regulatory protein, StAR, appears to be a molten globule. *Proc Natl Acad Sci USA* 96:7250–7255
- Hu MC, Guo IC, Lin JH, Chung BC 1991 Regulated expression of cytochrome P-450_{scc} (cholesterol-side-chain cleavage enzyme) in cultured cell lines detected by antibody against bacterially expressed human protein. *Biochem J* 274(Pt 3):813–817
- Hales DB, Sha LL, Payne AH 1987 Testosterone inhibits cAMP-induced *de novo* synthesis of Leydig cell cytochrome P-450(17 α) by an androgen receptor-mediated mechanism. *J Biol Chem* 262:11200–11206
- Medvinsky A, Smith A 2003 Stem cells: fusion brings down barriers. *Nature* 422:823–825
- O'Shaughnessy PJ, Willerton L, Baker PJ 2002 Changes in Leydig cell gene expression during development in the mouse. *Biol Reprod* 66:966–975
- Parker KL, Schimmer BP 1997 Steroidogenic factor 1: a key determinant of endocrine development and function. *Endocr Rev* 18:361–377
- Peng L, Arensburg J, Orly J, Payne AH 2002 The murine 3 β -hydroxysteroid dehydrogenase (3 β -HSD) gene family: a postulated role for 3 β -HSD VI during early pregnancy. *Mol Cell Endocrinol* 187:213–221
- Staels B, Hum DW, Miller WL 1993 Regulation of steroidogenesis in NCI-H295 cells: a cellular model of the human fetal adrenal. *Mol Endocrinol* 7:423–433
- Heim M, Frank O, Kampmann G, Sochocky N, Pennimpede T, Fuchs P, Hunziker W, Weber P, Martin I, Bendik I 2004 The phytoestrogen genistein enhances osteogenesis and represses adipogenic differentiation of human primary bone marrow stromal cells. *Endocrinology* 145:848–859
- Lo KC, Lei Z, Rao Ch V, Beck J, Lamb DJ 2004 *De novo* testosterone production in luteinizing hormone receptor knockout mice after transplantation of Leydig stem cells. *Endocrinology* 145:4011–4015
- De Bari C, Dell'Accio F, Tylzanowski P, Luyten FP 2001 Multipotent mesenchymal stem cells from adult human synovial membrane. *Arthritis Rheum* 44:1928–1942
- Crawford PA, Sadovsky Y, Milbrandt J 1997 Nuclear receptor steroidogenic factor 1 directs embryonic stem cells toward the steroidogenic lineage. *Mol Cell Biol* 17:3997–4006
- Bjorkhem I 2002 Do oxysterols control cholesterol homeostasis? *J Clin Invest* 110:725–730
- Pandak WM, Ren S, Marques D, Hall E, Redford K, Mallonee D, Bohdan P, Heuman D, Gil G, Hylemon P 2002 Transport of cholesterol into mitochondria is rate-limiting for bile acid synthesis via the alternative pathway in primary rat hepatocytes. *J Biol Chem* 277:48158–48164
- Gondo S, Yanase T, Okabe T, Tanaka T, Morinaga H, Nomura M, Goto K, Nawata H 2004 SF-1/Ad4BP transforms primary long-term cultured bone marrow cells into ACTH-responsive steroidogenic cells. *Genes Cells* 9:1239–1247

Leucine-Rich Repeat-Containing G Protein-Coupled Receptor-4 (LGR4, Gpr48) Is Essential for Renal Development in Mice

Shigeki Kato^a Mitsunobu Matsubara^b Tsuyoshi Matsuo^a Yasuaki Mohri^a
Ituro Kazama^b Ryo Hatano^b Akihiro Umezawa^c Katsuhiko Nishimori^a

^aLaboratory of Molecular Biology, Graduate School of Agricultural Science, Tohoku University, Sendai,

^bDivision of Molecular Medicine, Center for Translational and Advanced Animal Research, Tohoku University School of Medicine, Sendai, and ^cNational Research Institute for Child Health and Development, Tokyo, Japan

Key Words

G protein-coupled receptor, leucine-rich repeat-containing · Glycoprotein hormone receptor homology · Leucine-rich repeats · Renal hypoplasia

Abstract

Leucine-rich repeat-containing G protein-coupled receptor (LGR)-4 is a G protein-coupled receptor (GPCR) with a seven-transmembrane domain structure. LGRs are evolutionally and structurally phylogenetic, classified into three subgroups and are members of the so-called orphan receptors whose ligands have yet to be identified. We generated knockout mice lacking *Lgr4* (*Gpr48*) by targeted deletion of part of exon 18, which codes for the transmembrane and signal-transducing domains of the receptor. *Lgr4* null mice were born at much less than the 25% expected frequency from crosses of *Lgr4* heterozygous mice (*Lgr4*^{+/-}). *Lgr4* null mice that survived in utero died shortly after birth in almost all cases. We observed striking renal hypoplasia in the null mice, accompanied by elevated concentration of plasma creatinine. Histological analysis of the P0 null mouse kidney showed a notable decrease in the total number and density of the glomerulus. Thus, the function of *Lgr4* is essential to regulate renal development in the mouse. This study suggests that the *Lgr4* gene is a new and important member of LGRs involved in a group of genes responsible for hereditary disease in the kidney.

Copyright © 2006 S. Karger AG, Basel

Introduction

Leucine-rich repeat-containing G protein-coupled receptor 4 (*Lgr4*; *Gpr48*) was first identified as a novel G protein-coupled receptor with glycoprotein hormone receptor homology [1]. Glycoprotein hormone receptors, including the gonadotropin receptors follicle-stimulating hormone receptor [2] and luteinizing hormone/chorionic gonadotropin receptor [3], share conserved leucine-rich repeats in their first extracellular domains. These extracellular domains typically comprise more than half of the total protein amino acids. The receptors couple with intracellular Gs α -type G proteins, and their intracellular effects are mediated in large part by adenylate cyclase activity and the resulting increase in cellular cAMP levels. Although *LGR7* [4, 5] and *LGR8* [6, 7] were recently identified as receptors for relaxin [8–10], ligands for many other newly identified LGRs, including LGR4, are unknown; hence, LGR4 is classified among the orphan receptors. Ligands of the most well-characterized receptors, including follicle-stimulating hormone, luteinizing hormone, human chorionic gonadotropin, and thyroid-stimulating hormone, are heterodimeric in composition, consisting of the common α -subunit and the hormone-specific β -subunit. Ligands of the still orphan LGRs are presumed to be structurally related.

Mice deficient in the *Lgr4* gene are a potentially valuable tool to study the in vivo function of *Lgr4* and to ex-

KARGER

Fax +41 61 306 12 34
E-Mail karger@karger.ch
www.karger.com

© 2006 S. Karger AG, Basel
1660–2129/06/1042–0063\$23.50/0

Accessible online at:
www.karger.com/nee

Katsuhiko Nishimori
Laboratory of Molecular Biology, Graduate School of Agricultural Science
Tohoku University, 1-1 Tsutsumidori-Amamiyamachi, Aoba-ku
Sendai 981-8555 (Japan)
Tel. +81 22 717 8770, Fax +81 22 717 8883, E-Mail knishimo@mail.tains.tohoku.ac.jp

plore LGR4 candidate ligand(s). To address the physiological roles of mouse *Lgr4*, we deleted a part of exon 18 coding for the transmembrane and signal-transducing domains of LGR4 via homologous recombination in embryonic stem (ES) cells. We describe this herein, as well as our characterization of renal developmental phenotypes in *Lgr4* null mutant mice.

Materials and Methods

Northern Blot Analysis

Messenger RNA was extracted from different organs using RNA Stat 60 (Leedo Medical Laboratories, USA). Two micrograms of poly(A)⁺ RNA were electrophoresed, transferred onto nylon transfer membrane (Pall BioSupport, USA), and blocked before being used for hybridization. A [³²P]-dCTP-radiolabeled probe was generated from 440 bp of sequence corresponding to nucleotide (nt) 101 to 540 of mouse *Lgr4* mRNA (Amersham Biosciences, Japan) and applied to the blot under standard hybridization conditions. After washing, the blot was exposed to X-ray film (Kodak, Japan). The size of the transcripts was estimated using the positions of 18S rRNA, 28S rRNA and GAPD mRNA.

5' Primer Extension Analysis

Primer extension analysis was performed. Briefly, an IRD-800 (LI-COR, Japan)-labeled oligonucleotide complementary to bases from nt -211 to -193 of the coding strand (5'-GAAGGGAGAAACTGCGGAG-3') was hybridized overnight at 42°C with 15 µg total RNA from mouse ovaries. Hybridized samples were reverse transcribed into cDNA with Superscript III Reverse Transcriptase (Invitrogen, Japan). One microgram of RNase H (Invitrogen, Japan) was added, and the reaction was incubated at 37°C for 30 min. The resultant products were precipitated and run on a 6% denaturing polyacrylamide gel along with the corresponding sequence reactions.

Generation of *Lgr4*-Deficient Mice

The genomic targeting vector contained, in order, 7.5 kb of genomic sequence (including *Lgr4* exons 11–17), a 5'-loxP site, a P_{gk}Neo-expression cassette surrounded by FRT sites at both ends, a portion of exon 18, a 3'-loxP site, and 2.0 kb of genomic DNA downstream of the *Lgr4*-coding region (including an untranslated *Lgr4* mRNA sequence). An expression cassette for negative selection of non-homologous insertion MC1-tk was also added. E14Tg2a ES cells were electroporated with 25 µg of linearized targeting vector, and targeted clones were selected for using G418 and 1-(2-deoxy-2-fluoro-β-D-arabinofuranosyl)-5-iodouracil (FIAU; Moravak Biochemicals, USA). Clones with the desired homologous recombination events at both sides of the vector were identified by Southern blot analysis using a 5'-internal probe and 3'-external probe [11]. These ES cell clones were used for C57BL/6 blastocyst injection to generate germline transmission chimeras. We defined the *Lgr4*^{Floxed} allele as that with the intact targeting vector, and maintained heterozygous *Lgr4*^{Floxed} mice (*Lgr4*^{Floxed/+}) in a mixed 129 SvEvC57BL/6 genetic background. To obtain the *Lgr4* knockout or null allele, *Lgr4*^{Floxed/+} mice were crossed with CAG-Cre 'transgenic general deleter' mice [12]. Het-

erozygous mice (*Lgr4*^{+/-}) were then interbred to produce the null mice (fig. 3A). The Ethics Review Committee for Animal Experimentation of Tohoku University approved all experimental protocols described in the present study.

PCR Genotyping

PCR analysis was used for genotyping DNA obtained from tail samples. Genomic DNA was extracted by ethanol precipitation after proteinase K digestion in a tissue lysis buffer (50 mM Tris-HCl (pH 7.5), 50 mM EDTA (pH 8.0), 100 mM NaCl, 0.5 mM spermidine, 1% SDS, 5 mM DTT). Three primers were used to distinguish the mutated allele from the wild-type allele; they were designated: upstream primer 1 (5'-GCCACAAGGGAGGATAGAAATC-3'), upstream primer 2 (5'-CCCAGCAAGAGCTAGGAAAGA-3'), and downstream primer 3 (5'-GCCATCAAATCCCTTGGATA-3'). The wild-type allele gives a PCR amplicon of 608 bp using primers 1 and 3, while primers 2 and 3 generate a 345-bp product from the null allele.

Fertility Studies

We carried out timed mating by housing one male with one or two females for periods of at least 5 days. Every morning during this period, females were evaluated for the presence of vaginal plug. Embryonic gestation day 0.5 (E0.5) was defined by the presence of a copulation plug, whereas the day of birth was defined as P0. Pregnant heterozygous mice were sacrificed and fetuses were obtained at specific time points in embryonic development, E13.5, 14.5, 15.5, 16.5, 17.5, 18.5, and 19.5. Fetuses and newborns were weighed and sacrificed by decapitation to obtain tails for genotyping and kidneys for histological analysis. Blood was collected from the carotid arteries into 50 µl non-heparinized capillary tubes.

Histology

For renal histology, kidneys from postnatal mice were fixed in 4% paraformaldehyde overnight. After dehydration, they were embedded in paraffin. Paraffin blocks were sectioned at 2- to 5-µm thickness, and stained with hematoxylin-eosin, periodic acid-Schiff (PAS) and periodic acid silver-methenamine using standard procedures. In case of E13.5 kidneys, these were frozen with Tissue-Tek O.C.T. Compound (Sakura Finetechnical, Japan), sectioned at 6–10 µm, fixed, and further processed as described for the postnatal kidneys.

Blood Analysis

Plasma creatinine levels were measured by a chemical auto-analyzer (DRI-CHEM 3500V, Fuji Film, Japan). Breathing neonatal mice were decapitated and about 20 µl of blood was immediately corrected by a pipetteman. The blood sample was centrifuged (3,000 rpm) for 5 min at room temperature to prepare supernatant as plasma. Ten microliters of plasma sample were further processed with the autoanalyzer according to the manufacturer's protocol.

Nephron Density Studies

The numbers of nephrons per unit area (mm³) were counted. For each kidney collected, three (*Lgr4*^{-/-}) or four (*Lgr4*^{+/+} and *Lgr4*^{+/-}) different non-adjacent sections of the organ were used. Data were statistically analyzed.

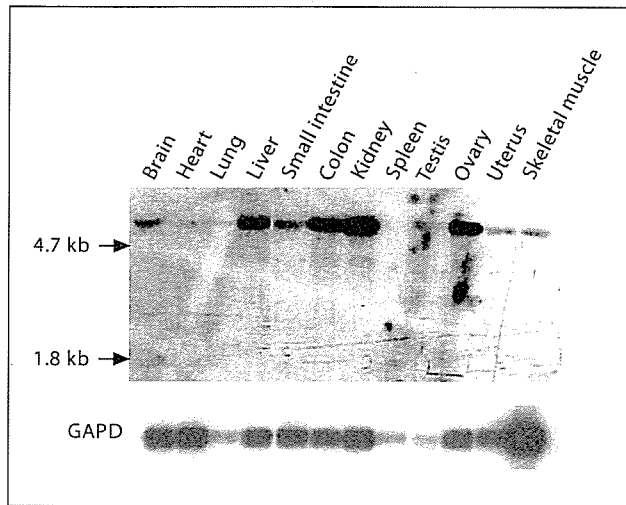


Fig. 1. Multi-tissue Northern blot analysis showing expression of *Lgr4* mRNA. Two micrograms of poly(A)⁺ RNA from various tissues of adult mice were hybridized with a [³²P]-labeled 440-bp *Lgr4* cDNA probe. A major message, approximately 5 kb in size, was detected in the kidney, ovary, colon, liver, and brain. The heart, lung, small intestine, testis, uterus and skeletal muscle showed relatively weak signals.

Statistical Evaluation

All experimental data are expressed as the means ± SEM. Individual comparisons were made between genotype groups using ANOVA followed by Student's t test. A p value of <0.05 was considered significant.

Results

Cloning of *Lgr4* cDNA and Tissue Distribution of *Lgr4* Transcript in Various Organs

To study the expression of *Lgr4* in wild-type adult mice, we performed Northern blot analysis. As shown in figure 1, a 5.0-kb *Lgr4* transcript was detected in multiple organs. The highest level of expression was seen in the kidney, followed by the ovary, colon, and liver (fig. 1). In contrast, the heart, lung, testis, uterus, and skeletal muscle showed relatively lower signal intensity, and no bands were detected corresponding to transcript in the pancreas or spleen.

Determining the m*Lgr4* Transcription Start Site

To identify the start site of transcription on the m*Lgr4* gene, 5'-primer extension analysis was performed, and we found that transcription was initiated at nt -255 with

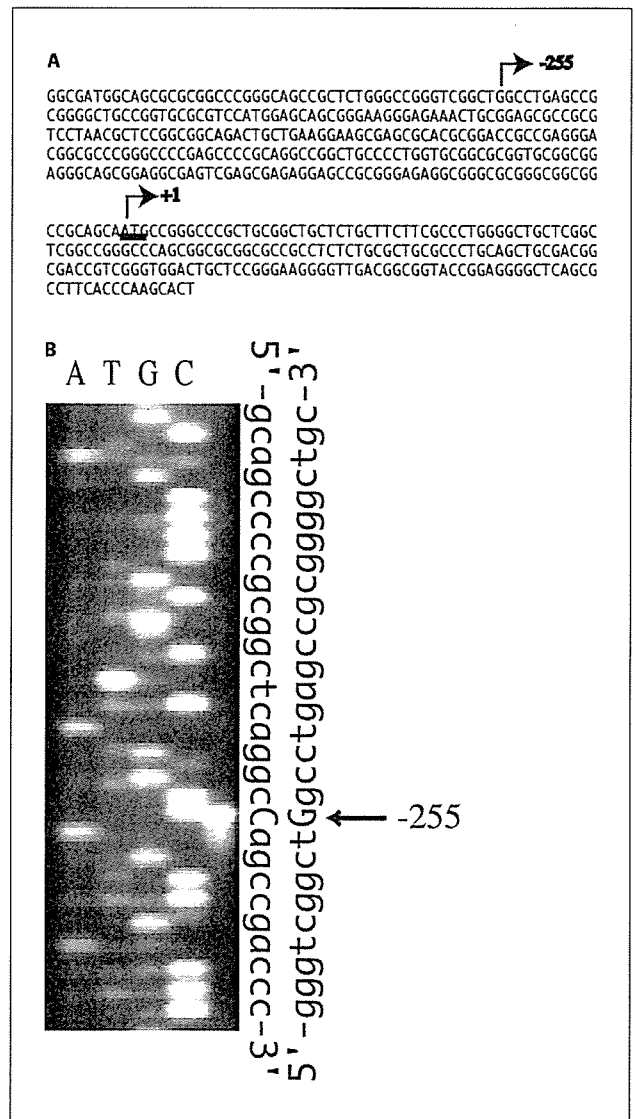


Fig. 2. Determination of the transcription start site of the m*Lgr4* gene. Primer extension analysis with 15 μg of ovary total RNA was done to determine the transcription start site of m*Lgr4*. The band indicates the start site at nt -255 relative to the translational start site.

respect to the translation initiation site (fig. 2). This allows correct description of *Lgr4* exon 1 (440 bp; fig. 3A).

Construction of the Gene-Targeting Vector and Generation of *Lgr4*-Deficient Mice

To generate a targeting construct, a 7.5-kb fragment spanning from exon 11 to exon 17 was used as a 5'-arm

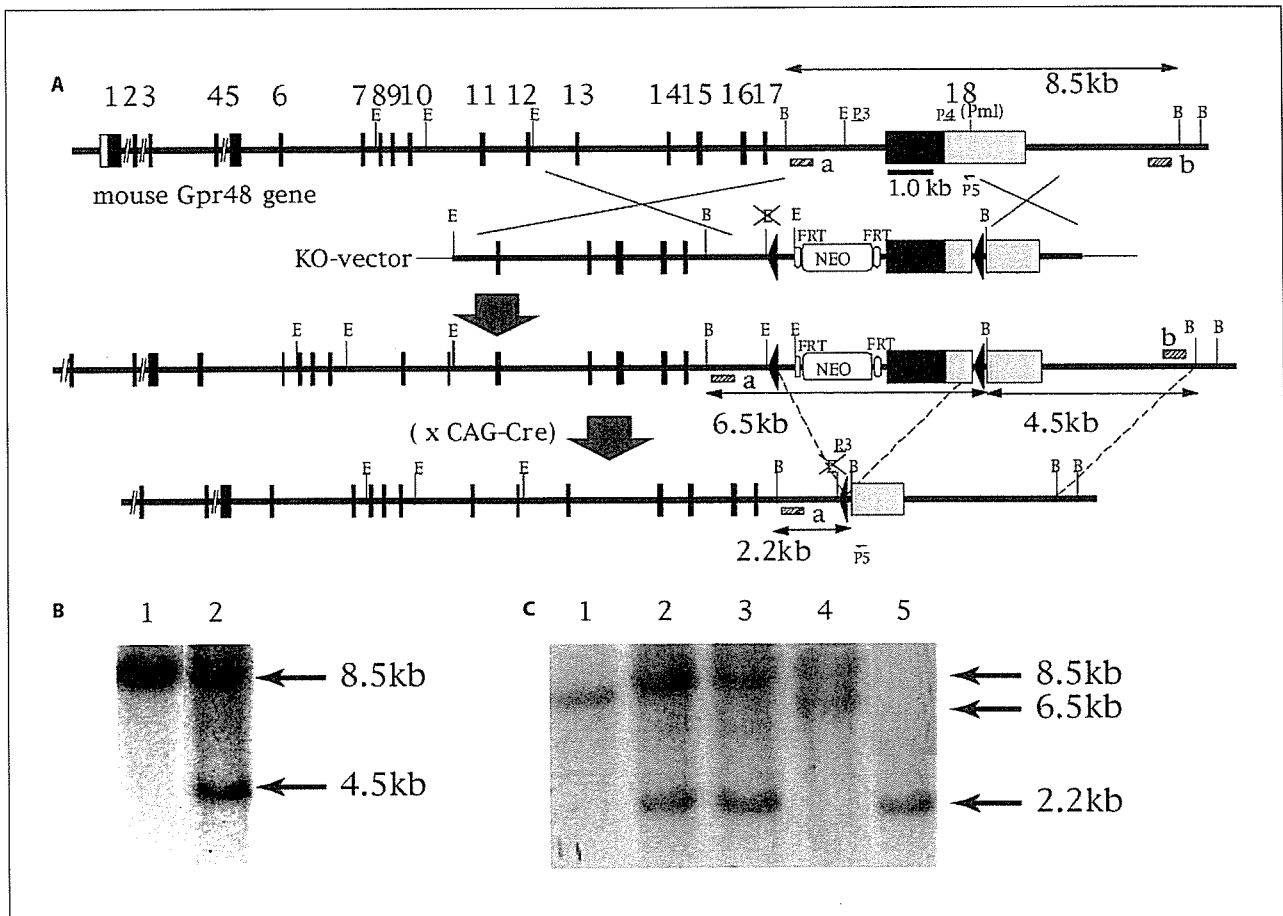


Fig. 3. Construction of the *Lgr4* gene knockout vector, and the generation and characterization of *Lgr4* gene-deficient mice. **A** The wild-type *mLgr4* allele and the deletion-targeting vector are shown. The targeted domain includes a 2.2-kb sequence comprising half of exon 18. A schema of the targeted allele after homologous recombination and the recombined allele after Cre-mediated excision followed. Black boxes and gray boxes indicate the translated regions and non-translated regions in exons, respectively. Triangles and ellipses are *loxP* and FRT sites, respectively. Exons are numbered. Interruptions within intron-1, intron-2 and intron-4 by double slash lines represent the long intron spanning 52.4, 18.9 and 5.4 kb, respectively. B = *Bam*HI; E = *Eco*RI. **B** Ge-

nomonic DNA was prepared from ES cell clones and digested with *Bam*HI for analysis by Southern hybridization with probe 'b'. DNA was run on lanes 1 and 2. Lane 1 shows a non-targeted cell and lane 2 shows correct homologous recombination cell. **C** Tail DNA was used for Southern blot hybridization with probe 'a'. The picture shows results for wild-type mice (+/+; lane 1), heterozygous mice (+/-; lanes 2 and 3), Floxed mice (Floxed/+; lane 4) and the null mice (-/-; lane 5). Southern analyses with 5' internal probe 'a' and 3' external probe 'b', drawn by striped bars, were carried out to detect the correct recombination in *mLgr4* locus of ES cell clones and resultant mice.

of homology, and a 2.0-kb fragment spanning the end of exon 18 and the 3'-UTR was used as a 3' arm of homology (fig. 3A). An intervening portion of exon 18 with flanking *loxP* sites (Floxed allele) was used to allow Cre recombinase-mediated deletion of part of this exon, deleting the LGR4 transmembrane domain and signal-transducing coding sequences (null allele; fig. 3A).

The targeting vector was linearized and electroporated into E14Tg2a ES cells as described previously [11, 13]. Approximately 400 G418 and FIAU-resistant colonies were screened by Southern blot analysis with an internal probe (shown as probe 'a' in fig. 3A). This probe recognizes 8.5- and 6.5-kb bands corresponding to the wild-type and targeted alleles, respectively. Confirmation of

the targeted clones was performed by Southern blot analysis with an external probe (shown as probe 'b' in fig. 3A) that recognized a 8.5-kb band wild-type allele, and 4.5-kb fragment corresponding to the Floxed allele (fig. 3B).

Four ES cell clones were found to be correctly targeted, corresponding to a targeting frequency of 1% in clones surviving selection. These were microinjected into C57BL/6 mouse blastocysts to generate chimeras. One chimera gave germline transmission, and was crossed with the CAG-Cre general deleter mouse [12] to remove the transmembrane coding sequence of the *Lgr4* gene and thus establish the heterozygous *Lgr4* mouse line. To confirm the deletion, tail DNA was prepared for genomic Southern blot analysis using the internal probe 'a'. We identified the newly generated 2.2-kb band corresponding to the null allele after excision exon 18 (fig. 3C).

Lethality in *Lgr4* Null Mice

We genotyped pups at birth (P0) to estimate the ratio of wild-type and mutant *Lgr4* mice at birth (table 1B). Against the number of wild-type pups (n = 1,344), calculation with numbers from Mendelian expectation showed that 87.4% (n = 2,349) heterozygous and only 50.4% (n = 677) null pups were born. These data suggest embryonic loss of null mice.

Almost all of the newborn *Lgr4* null mice died within 2 days of birth (by day P2). Examination of their digestive organs revealed no evidence of suckling milk in contrast to their healthy littermates. One of the 2,105 pups surviving at weaning (P21) was a viable *Lgr4* null homozygous (table 1C); it showed severe growth retardation associated with death at P42 (see below).

To confirm the embryonic lethality of mutant mice, pregnant heterozygous females were sacrificed after timed mating with a heterozygous male for fetal genotyping between embryonic days E14.5 and E18.5. As shown in table 1A, the expected Mendelian frequency (wild-type:heterozygote:homozygote = 1:2:1) was maintained until E15.5; the numbers of heterozygous and null fetuses were measurably decreased after E16.5 and E18.5, respectively. Progressive loss of null mice continued throughout the E16.5–E18.5 interval. These data confirm the late embryonic lethality of the *Lgr4* null embryos. There were no statistical differences in lethality between sexes.

Gross Morphological Abnormalities of *Lgr4* Null Mice

Tables 2 and 3 show body and organ weights among wild-type and mutant embryos aged E14.5–E19.5. There

Table 1. Number of embryos at each embryonic day, and of newborn and weaned pups

A Number of embryos on each day					
	E14.5	E15.5	E16.5	E17.5	E18.5
+/+	36	31	38	30	33
+/-	68	65	73	55	50 ^a
-/-	33	32	25 ^a	21 ^a	18 ^b
B Number of pups at birth (P0, n = 4,370)					
+/+ 1,344	+/- 2,349 ^a		-/- 677 ^b		
Male 661	Male 1,187 ^a		Male 330 ^b		
Female 683	Female 1,162 ^a		Female 343 ^b		
C Number of pups at weaning (P21, n = 2,105)					
+/+ 784	+/- 1,320 ^a		-/- 1 ^b		
Male 382	Male 666 ^a		Male 1 ^b		
Female 402	Female 654 ^a		Female 0 ^b		

^a p < 0.05, -/- vs. +/+. ^b p < 0.01, -/- vs. +/+.

were no significant differences between the body weights of heterozygous *Lgr4*^{+/-} and wild-type littermates over this interval. In contrast, *Lgr4* null mice showed a significant decrease in body weight on each embryonic day compared to heterozygous or wild-type siblings. The weight reduction of most organs in null animals reflected the proportional change in the order of whole body weight reduction (maintaining 70% of wild-type counterpart weights). However, among the organs analyzed, a more striking hypoplasia was noted in renal tissues, with the average kidneys contributing 0.51% overall to the total body weight in wild-type and *Lgr4*^{+/-} mice, and 0.23% in the null mice (table 3).

Kidney Abnormalities in *Lgr4* Null Mice

The normal kidney shows the highest expression on the *Lgr4* transcript (fig. 1), and renal weights were found to be severely reduced in *Lgr4* null mice. These findings indicate that the kidney would be the most severely affected organ in the absence of a functional *Lgr4* gene. Therefore, we focused our studies of *Lgr4*^{-/-} mice on renal pathology.

Almost all of the *Lgr4* null mice died within 2 days of birth; one exception being a single mouse that survived to 6 weeks of age. The body weight of this survivor reached only 5.0 g at P28, while the weight of its littermates in-

Table 2. Overview of absolute embryonic body weights (g) in wild-type (+/+), heterozygous (+/-) and null (-/-) mice

	E14.5	E15.5	E16.5	E17.5	E18.5	E19.5
+/+	0.31 ± 0.02 (n = 24)	0.44 ± 0.02 (n = 25)	0.59 ± 0.02 (n = 26)	0.79 ± 0.02 (n = 23)	0.96 ± 0.01 (n = 27)	1.28 ± 0.01 (n = 21)
+/-	0.28 ± 0.01 (n = 48)	0.43 ± 0.01 (n = 44)	0.56 ± 0.01 (n = 41)	0.83 ± 0.02 (n = 52)	0.93 ± 0.02 (n = 45)	1.29 ± 0.02 (n = 39)
-/-	0.24 ± 0.02 (n = 21)	0.28 ± 0.02 (n = 23) ^a	0.46 ± 0.02 (n = 14) ^a	0.61 ± 0.02 (n = 14) ^b	0.79 ± 0.03 (n = 17) ^b	0.94 ± 0.03 (n = 13) ^b

Numbers tested are shown in parentheses with each data.

^a p < 0.05, -/- vs. +/+ and +/-; ^b p < 0.01, -/- vs. +/+ and +/-.

Table 3. Overview of absolute organ weights and organ weight/body weight ratios in wild-type (+/+), heterozygous (+/-) and null (-/-) mice at birth (mean ± SEM)

Organ and units	Genotype		
	+/+	+/-	-/-
Body weight, g	1.55 ± 0.02 (n = 64)	1.54 ± 0.01 (n = 121)	1.08 ± 0.02 (n = 44) ^a
%	100	100	100
Liver, mg	54.64 ± 0.94 (n = 61)	54.87 ± 0.75 (n = 112)	35.54 ± 0.96 (n = 36) ^a
%	3.525 ± 0.02	3.563 ± 0.02	3.291 ± 0.03
Spleen, mg	3.64 ± 0.08 (n = 61)	3.69 ± 0.05 (n = 112)	2.58 ± 0.12 (n = 36) ^a
%	0.234 ± 0.02	0.240 ± 0.01	0.239 ± 0.02
Heart, mg	11.13 ± 0.19 (n = 61)	11.09 ± 0.14 (n = 112)	8.23 ± 0.25 (n = 36) ^a
%	0.718 ± 0.02	0.720 ± 0.01	0.762 ± 0.04
Lung, mg	41.63 ± 0.78 (n = 61)	40.75 ± 0.68 (n = 112)	31.20 ± 0.75 (n = 36) ^a
%	2.686 ± 0.02	2.646 ± 0.02	2.889 ± 0.05
Kidney, mg	7.99 ± 0.13 (n = 61)	7.81 ± 0.07 (n = 112)	2.43 ± 0.11 (n = 36) ^a
%	0.515 ± 0.02	0.507 ± 0.02	0.225 ± 0.07 ^a
Testis, mg	0.88 ± 0.04 (n = 31)	0.83 ± 0.02 (n = 57)	0.69 ± 0.03 (n = 18) ^b
%	0.057 ± 0.01	0.054 ± 0.01	0.064 ± 0.01
Adrenal, mg	0.43 ± 0.01 (n = 47)	0.45 ± 0.01 (n = 79)	0.36 ± 0.01 (n = 28) ^a
%	0.028 ± 0.007	0.029 ± 0.007	0.033 ± 0.008

Organ weight/body weight ratios are given as percent. Numbers tested are shown in parentheses with each data.

^a p < 0.01, -/- vs. +/+ and +/-; ^b p < 0.05, -/- vs. +/+ and +/-.

creased to approximately 15.0 g (fig. 4A). The kidneys of the null mouse were recovered just after it died and showed multiple fluid-filled cystic lesions (fig. 4B–D). On histological analysis, tubular epithelial cells appeared flattened, and vacuolar degeneration of these cells was pronounced. Proteinaceous debris can be seen inside the cystic lesions. The numbers of glomeruli were marked decreased. The remaining glomeruli did not show sig-

nificant structural alteration by PAS stain, suggesting that their loss may be secondary to injury in the tubular nephron compartments. These findings are reminiscent of the histological hallmarks of human polycystic kidney disease and suggest a possible relationship between the *Lgr4* gene and this disorder (considered in the Discussion below).